buildings

MDPI

Article

A Two-Stage Generative Optimization Framework for "Daylighting Schools": A Case Study in the Lingnan Region of China

Haoming Song [1,2], Yubo Liu [1,2,*] and Qiaoming Deng [1,2]

[1] School of Architecture, South China University of Technology, Guangzhou 510641, China; arhaoming@mail.scut.edu.cn (H.S.); dengqm@scut.edu.cn (Q.D.)
[2] State Key Laboratory of Subtropical Building and Urban Science, Guangzhou 510641, China
* Correspondence: liuyubo@scut.edu.cn

Abstract

Within the framework of the Healthy China strategy, daylighting in primary and secondary schools is crucial for students' health and learning efficiency. Most schools in China still face insufficient and uneven daylighting, along with limited outdoor solar exposure, underscoring the need for systematic optimization. Guided by the "Daylighting School" concept, this study proposes a campus design model that integrates indoor daylighting with outdoor activity opportunities and explores a generative optimization approach. The research reviews daylighting and thermal performance metrics, summarizes European and American "Daylighting School" experiences, and develops three classroom prototypes—Standard Side-Lit, High Side-Lit, and Skylight-Lit—together with corresponding campus layout models. A two-stage optimization experiment was conducted on a high school site in Guangzhou. Stage 1 optimized block location and functional layout using solar radiation illuminance and activity accessibility distance. Stage 2 refined classroom configurations based on four key performance indicators: sDA, sGA, UOD, and APMV-mean. Results show that optimized layouts improved activity path efficiency and daylight availability. High Side-Lit and Skylight-Lit classrooms outperformed traditional Side-Lit in illuminance, uniformity, and glare control. To improve efficiency, an ANN-based prediction model was introduced to replace conventional simulation engines, enabling rapid large-scale assessment of complex classroom clusters and providing architects with real-time decision support for daylight-oriented educational building design.

Keywords: Daylighting School; classroom design; generative design; multi-objective optimization; artificial neural network

check for updates

Academic Editor: Vincenzo Costanzo

Received: 14 September 2025
Revised: 13 October 2025
Accepted: 16 October 2025
Published: 23 October 2025

Citation: Song, H.; Liu, Y.; Deng, Q. A Two-Stage Generative Optimization Framework for "Daylighting Schools": A Case Study in the Lingnan Region of China. *Buildings* **2025**, *15*, 3821. https://doi.org/10.3390/buildings15213821

Copyright: © 2025 by the authors. Licensee MDPI, Basel, Switzerland. This article is an open access article distributed under the terms and conditions of the Creative Commons Attribution (CC BY) license (https://creativecommons.org/licenses/by/4.0/).

1. Introduction

In recent years, with increasing academic pressure and fierce competition for university entrance examinations, Chinese primary and secondary school students spend an exceptionally long time in classrooms [1]. At the same time, rapid urbanization in recent decades has intensified the shortage of campus space [2]. With the national urbanization rate rising to nearly 70%, large populations have concentrated in cities, driving a sharp increase in school enrollment demand. However, limited urban land supply and high development intensity have resulted in significantly lower per capita campus area compared to international standards. For example, in the United States, the average campus area per student ranges from 12.4 to 18.5 m^2 [3], which is two to three times higher than in

China [4]. As a consequence, students in Chinese schools often lack sufficient exposure to natural daylight both indoors and outdoors. Teaching buildings in densely populated urban areas are increasingly compressed, leading to inadequate daylighting in classrooms, while playgrounds and sports facilities are often too limited to support adequate outdoor activity. Therefore, under such high-density development conditions, improving classroom daylighting quality and optimizing campus spatial design have become urgent priorities in educational architecture.

1.1. Research Questions and Solution

1.1.1. Indoor: Uneven Natural Light Distribution and Insufficient Illuminance

Natural light is essential for children's health, regulating circadian rhythms, improving mood, and preventing myopia [5–8]. Yet over 50% of Chinese adolescents are myopic [9], and classrooms often suffer from insufficient illuminance, uneven distribution, and glare [10–15]. A common issue is excessive brightness near windows contrasted with inadequate illuminance in areas farther away, leading to pronounced luminance differences that not only reduce visual comfort but also aggravate eye fatigue.

Evidence from multiple countries confirms this problem. Surveys in the Netherlands and Greece show that many students are disturbed by direct sunlight and glare, often resorting to blinds and artificial lighting [16,17]. Similar findings in China reveal that, although average illuminance often meets standards, spatial disparities are significant, with window-side seats experiencing severe glare [18–20]. In the Lingnan region in China, some schools even depend on the practice of "drawing blinds and turning on lights" during daytime to balance illuminance, which reduces daylight utilization and increases energy consumption (Figure 1a). Direct sunlight-induced glare also causes temporary visual impairment, distraction, and fatigue, affecting both students and teachers [21–23].



(**a**) (**b**)

Figure 1. (**a**) Common daylighting issue: lights on and curtains closed due to glare; (**b**) Limited student activity in corridors due to distant or elevated playgrounds.

1.1.2. Outdoor: Limited Opportunities for Sunlight Exposure

Outdoor sunlight exposure during school hours is equally critical for students' visual health. Evidence shows that the duration of outdoor activity, rather than light intensity alone, is a key protective factor against myopia [24,25]. Moderate sunlight combined with physical activity can regulate refractive development and delay myopia progression [26,27]. To address this, China launched the "Sunshine Sports Program" in 2007, recommending at least one hour of outdoor exercise daily [28]. Yet, by 2022, junior high students averaged only 47 min per day—far below the international standard of two hours [29].

This shortfall results from multiple constraints, including fragmented recess time, safety concerns that relocate activities indoors, heavy academic loads, and inconvenient sports facilities (Figure 1b). A key solution lies in integrating campus planning with architectural design. A thoughtful layout of teaching buildings and athletic facilities can maximize students' incidental exposure to sunlight during breaks and transits between classes, enhancing their well-being without demanding extra time.

1.1.3. "Daylighting School": A Solution for Both Indoor and Outdoor Challenges

Since the 1990s, the Lighting Research Center (LRC) in the United States has taken the lead in exploring sustainable daylighting practices. In 2004, Professor Russell P. Leslie initiated the Daylighting Dividends program [30] and subsequently collaborated with multiple organizations to compile the *Guidelines for Daylighting Schools* [30], which introduced the concept of the "*Daylighting School*". In 2010, he further published *Patterns to Daylight Schools for People and Sustainability* [31], systematically summarizing pattern-based strategies for school daylighting design and providing The accumulated research experience can be summarized in two main aspects (Table 1).

Table 1. Design Principles Summarized in the *Guidelines for Daylighting Schools*.

Type	Design Principle	Interpretation
Activity Space	① Locate Outdoor Activity Areas Near Classrooms	Ensure outdoor spaces are easily accessible during breaks to encourage sunlight exposure and spontaneous outdoor activity.
	② Provide Open-Air Platforms for Multi-Level Classrooms	Use stepped or staggered layouts to allow each classroom direct access to an adjacent open-air platform.
Classrooms	① Prioritize Natural Daylighting	Ensure sufficient daylight to reduce reliance on artificial lighting.
	② Avoid Direct Sunlight	Control solar penetration to reduce glare and improve comfort.
	③ Ensure Uniform Light Distribution	Design for even daylight to enhance visual comfort and learning efficiency.
	④ Differentiate Daylighting and View Windows	Use high-positioned windows for daylighting; low windows for views only. Avoid relying on view windows as primary light sources.
	⑤ Integrate Daylighting Early	Embed daylighting strategies at the design inception for optimal performance and cost-efficiency.

- **First, classroom daylighting patterns.** By integrating design elements such as roofs, skylights, side windows, and light shelves, classrooms can achieve sufficient illumination, balanced distribution, and controlled glare. For instance, in European and American "Daylighting School" cases such as Smith Middle School (Figure 2a) and North Guilford Middle School (Figure 2b), reflective panels, grids, and skylights were applied collaboratively to avoid direct glare while enhancing uniformity. Compared with the prevailing reliance on single-side windows in China, such strategies demonstrate stronger sustainability and adaptability.
- **Second, campus layout and outdoor activity spaces.** Rational campus planning can shorten the distance between classrooms and outdoor areas, thereby increasing students' access to natural light. Historical examples in Europe and the U.S., such as Corona School (Figure 2c) and Munkegård School (Figure 2d), commonly adopted low-rise "carpet-type" layouts in which each classroom was connected to an independent outdoor activity area. This approach not only prolonged outdoor activity time but also improved indoor ventilation.



(**a**) (**b**) (**c**) (**d**)

Figure 2. (**a**) Classroom of Smith Middle School with "skylight aperture + louver" design [32]; (**b**) Classroom at North Guilford Middle School featuring a suspended barrel-vault light shelf [33]; (**c**) Open-air activity platform adjacent to classrooms at Corona School [34]; (**d**) Private courtyard provided for each classroom at Munkegård School [35,36].

1.2. Research Challenge

It is important to emphasize that the analysis of historical design experience in Europe and the United States aims not to replicate their design methods but to draw upon the refined design strategies, clear daylighting goals, and rigorous performance standards embodied in the "Daylighting School" concept. The educational context in China presents unique conditions—students spend longer hours in school, face greater academic intensity, and thus have a more urgent need for high-quality daylight environments. However, in the past, many advanced daylighting strategies were difficult to implement due to economic and technological constraints. With the improvement in construction technologies and technical capacities, systems such as skylights and reflective shading devices are no longer major obstacles. Consequently, the challenge in daylighting design in China has shifted from "whether it can be achieved" to "how well it can be achieved".

The core of localization lies in setting precise daylighting objectives based on regional climatic characteristics. Given China's vast territory, daylight conditions vary significantly. For example, northern regions require maximized daylight penetration during the short winter days, while the Lingnan region—where this study is based—faces the complex challenge of maintaining adequate illuminance while strictly controlling glare and solar heat gain under high humidity and large seasonal variations in solar altitude. Compared with other regions, this presents a higher level of optimization difficulty. To address this, the study dynamically simulates illuminance, uniformity, and glare performance. By optimizing shading systems and daylight control strategies, the design achieves stable and efficient daylighting performance throughout the year, making the "Daylighting School" concept measurable, operable, and adaptable to local contexts.

In terms of design methodology, it is equally essential to account for the architectural characteristics and teaching scale of Chinese schools. The "New Gaokao" reform and the emergence of flexible "class-based" teaching modes have introduced new spatial and functional requirements for classrooms and circulation areas. More critically, the widespread large-class system (40–60 students per class) in China results in deeper and longer classrooms than those in Western schools, where small-class teaching is common. In such deep spaces, traditional single-side windows often fail to ensure uniform light distribution, leaving rear zones inadequately illuminated. Therefore, the adoption of high side windows, skylights, and light-directing panels as part of hybrid daylighting systems becomes crucial to enhance light distribution and overall indoor lighting quality.

In summary, promoting the localization of the "Daylighting School" concept requires adherence to its core principles while closely integrating regional climate conditions, architectural typologies, and educational needs in China. We seek to establish a context-sensitive pathway for optimizing natural light in Chinese primary and secondary schools.

1.3. Research Aim

Achieving both high-quality daylighting and design feasibility in a "Daylighting School" poses significant challenges. This study addresses three key issues:

- **Develop a scientific daylighting evaluation system beyond window-to-floor ratio.**

In China, the window-to-floor ratio is widely used as criterion for assessing classroom daylight design. While simple to apply, it fails to capture the dynamic annual distribution and comfort of natural light. To address this, the present study introduces dynamic daylighting metrics (sDA, sGA) and develops a multidimensional evaluation system that is both more scientific and practical, providing reliable benchmarks for early-stage design [37].

- **Apply generative optimization to resolve multi-objective design conflicts.**

Classroom daylighting involves multiple and often conflicting objectives—including illuminance, uniformity, glare control, and spatial configuration—where design variables are numerous and interdependent. Conventional experience-based approaches cannot adequately balance these factors or predict light performance. This research establishes parametric generative rules and incorporates multi-objective optimization algorithms to automatically map design parameters to performance targets. Under defined boundary conditions, optimal solutions can be generated and filtered rapidly, thereby improving both efficiency and scientific rigor in design.

- **Use ANN models to reduce computation and enable large-scale assessment.**

"Daylighting School" projects often encompass multiple teaching blocks and numerous classrooms, requiring holistic simulation of daylight performance across clusters. Traditional simulation methods struggle to balance accuracy and scalability, resulting in high computational costs and delayed feedback. To overcome this, the study develops an artificial neural network (ANN)-based predictive model to partially replace conventional simulation engines. This approach significantly reduces computational load while enabling efficient large-scale daylighting assessment and optimization.

2. Literature Review

Artificial intelligence has been widely applied to the generation of campus and educational building layouts. As shown in Table 2, for performance-oriented daylighting design, diverse approaches have been developed across different climatic regions. International and domestic studies have integrated ANN, PSO, GA, and MADRL methods to optimize parameters such as window-to-wall ratio, shading, ceiling type, building massing, and material properties for classrooms, dormitories, libraries, and urban blocks. Evaluation metrics include sDA, UDI, ASE, UOD, PMV, UTCI, and EUI, with reported prediction accuracies generally high (R^2 0.8–0.99) [38–45]. Most of these works rely on simulation platforms such as Ladybug, Honeybee, and DIVA to generate large-scale training samples, which are then coupled with deep learning or evolutionary algorithms for efficient performance prediction.

Table 2. AI-Based Generative Design Studies in Architecture—Daylighting Performance-Oriented.

Algorithm	Application Context	Author(s)/Year	Simulation Tools	Decision Parameters	Optimization Objectives	Performance Metrics
MADRL-MATD3	Open-air Classroom (Subtropical Monsoon)	Liu et al. [38] (2023)	Ladybug v1 tools	Classroom dimensions, skylight/clerestory parameters, corridor parameters, relative position	sDA, ASE, UDI, PMV, OPA	RMSE [0.07, 2.44] MAE [0.05, 1.75] R^2 [0.81, 0.99]

Table 2. *Cont.*

Algorithm	Application Context	Author(s)/Year	Simulation Tools	Decision Parameters	Optimization Objectives	Performance Metrics
ANN-GA	Classroom/Academic Building (Subtropical Monsoon)	He [39] (2023)	Honeybee v0.0.65	Form parameters, ceiling parameters, side window parameters, shading parameters	DF, $UDI_{300–3000}$, $UDI_{<300}$, $UDI_{>3000}$	RMSE [0.61, 4.13] MAE [0.38, 2.90] R^2 [0.88, 0.97]
CycleGAN/pix2pix	Urban Block (Temperate Oceanic)	Huang et al. [40] (2022)	Ladybug, Eddy3d v0.4, OpenFOAM v22	Site boundary, block typology, opening position/distance, transformation/rotation, building dimensions	PLW, Radiation, UTCI	PLW-R^2 [0.70] Radiation-R^2 [0.86] UTCI-R^2 [0.80]
AdaBoost Regression	Residential Area (Subtropical Monsoon)	Zhang et al. [41] (2022)	Butterfly v1, Swift v4, Eddy3D, ixCube CFD 2020	Building geometry (height, shape, density, etc.)	Wind velocity ratio, UTCI	Wind Velocity: R^2 = 0.89 UTCI: R^2 = 0.99
ANN-GA	Residential Area (Tropical Monsoon)	Le-Thanh et al. [42] (2022)	DIVA v4	Material/Reflectance	UDI	RMSE [1.34, 7.62] MAE [0.01, 0.04] R^2 [0.89, 0.99]
PCA-ANN	Dormitory Building (Temperate Continental)	Razmi et al. [43] (2022)	Honeybee	Form parameters, corridor parameters, shading parameters	HLE, UDI, PTC	$R^2 > 0.99$
PSO-ANN	Library (Temperate Monsoon)	Sun et al. [44] (2020)	EnergyPlus v1, Radiance v1, Daysim v3	Building envelope, facade window width, skylight parameters	EUI, sDA, UDI, BEC	MAE [0.0009, 0.001] R^2 [0.97, 0.98]
CBDM-ANN	Classroom/Academic Building (Temperate Oceanic)	Lorenz et al. [45] (2020)	DIVA	Atrium geometry, orientation, Window-to-Wall Ratio (WWR)	DA, sDA	RMSE [0.33, 0.86] MAE [0.28, 0.53]

As shown Table 3, in primary and secondary school research, researchers have used models such as Pix2Pix and House-GAN++ to generate campus plans, which are then evaluated against indicators including floor area, density, and functional ratios. Other studies have employed multi-agent systems, genetic algorithms, and shape grammars to achieve end-to-end optimization, from massing generation to design evaluation [46–53]. Overall, these studies have advanced intelligent exploration of campus functional layouts but remain largely confined to spatial form and organizational structures.

Table 3. AI-Based Generative Design Studies of Chinese School Buildings—Function Layout-Oriented.

Algorithm(s)	Generated Object	Authors	Objectives & Methods
Pix2Pix (GAN), House-GAN++ (GNN)	University Campus Layout	Zhang [46] (2023)	Generated diverse layouts based on three types of constraints: functional zone connectivity, campus axes, and the relative positions of functional zones. Evaluated results using five quantitative metrics: diversity, controllability, site scale, functional area ratios, and building density/FAR.
Genetic Algorithm, Multi-Agent System (MAS), Graph Theory, Mathematical Programming	K-12 School Campus Layout	Li [47] (2025)	Proposed a layout generation method based on a multi-objective genetic algorithm, integrating MAS, shape grammars, and mathematical programming to create a comprehensive design workflow. The system evaluates solutions based on building form and environmental factors.

Table 3. *Cont.*

Algorithm(s)	Generated Object	Authors	Objectives & Methods
Graph Theory, Matrix Operations	K-12 School Campus Layout	Shi [48] (2023)	Explored algorithmic generation based on corridor-style spatial rules. The method utilizes: (1) Binary coding and matrix operations for layout prototyping; (2) Graph theory to define topological constraints; (3) Integer programming for room arrangement.
Pix2Pix (GAN)	Primary School Campus Layout	Lin [49] (2222)	Compared generated layouts against conventional design principles and building codes. The model demonstrated good performance in replicating traditional layout patterns, achieving target density/FAR, and satisfying rules for building orientation, acoustic separation, and main entrance placement.
Pix2Pix (GAN)	University Campus Layout	Lai [50] (2021)	Trained a pix2pix model on a central ring-road campus archetype. The model successfully generated rational layouts as color-coded "spatial organization maps," which require further interpretation and design development by architects.
Multi-Agent System (MAS), Mathematical Programming	K-12 School Campus Layout	Zhang [51] (2018)	Investigated form and space generation under environmental and functional constraints. The method combines a MAS for rule-based form generation with integer programming for optimizing spatial layout according to program requirements.
CAS Multi-Agent System	K-12 School Campus Layout	Ma [52] (2020)	Developed a layout tool using the self-organizing capabilities of agents to satisfy multiple constraints, including building separation, functional clustering, site boundaries, program requirements, egress distances, and natural daylighting.
Rule-Based System	K-12 School Campus Layout	Liang [53] (2020)	Developed a semi-automated design tool that generates and optimizes building massing based on a "rule system" and modular algorithms. The system assists architects by providing climate-optimized massing options to inform design decisions.

The existing literature on daylighting in primary and secondary schools can be grouped into two categories. The first focuses on classroom interiors from a technical perspective, optimizing illuminance, uniformity, and visual comfort through window design strategies, and material selection (Table 2). The second focuses on architecture design, examining orientation, massing, and spacing within school clusters to improve overall solar access (Table 3). However, these two approaches are typically pursued in isolation, lacking systematic integration. As a result, interior optimization outcomes often fail to translate effectively into campus-level design. In reality, the daylighting quality of individual classrooms is closely tied to campus-scale configurations. Sunlight affects not only learning environments but also the accessibility and usability of outdoor activity spaces.

Therefore, this study aims to establish a coupling framework between the micro scale (classroom light and thermal environments) and the macro scale (campus layout), exploring an integrated approach to "holistic daylight environments" that simultaneously addresses indoor daylighting performance and outdoor activity accessibility.

3. Research Method

3.1. Workflow

The experiment is conducted under the climatic conditions of the Lingnan region in China, with the goal of creating a "Daylighting School". A high school site in Guangzhou was selected as the case study, focusing on generative optimization of teaching blocks and classroom clusters. The integration of a genetic algorithm (GA) enables multi-objective optimization of school design, effectively balancing daylight availability, glare control, and thermal comfort, which traditional single-objective approaches fail to achieve. The optimization process is divided into two stages (Figure 3).

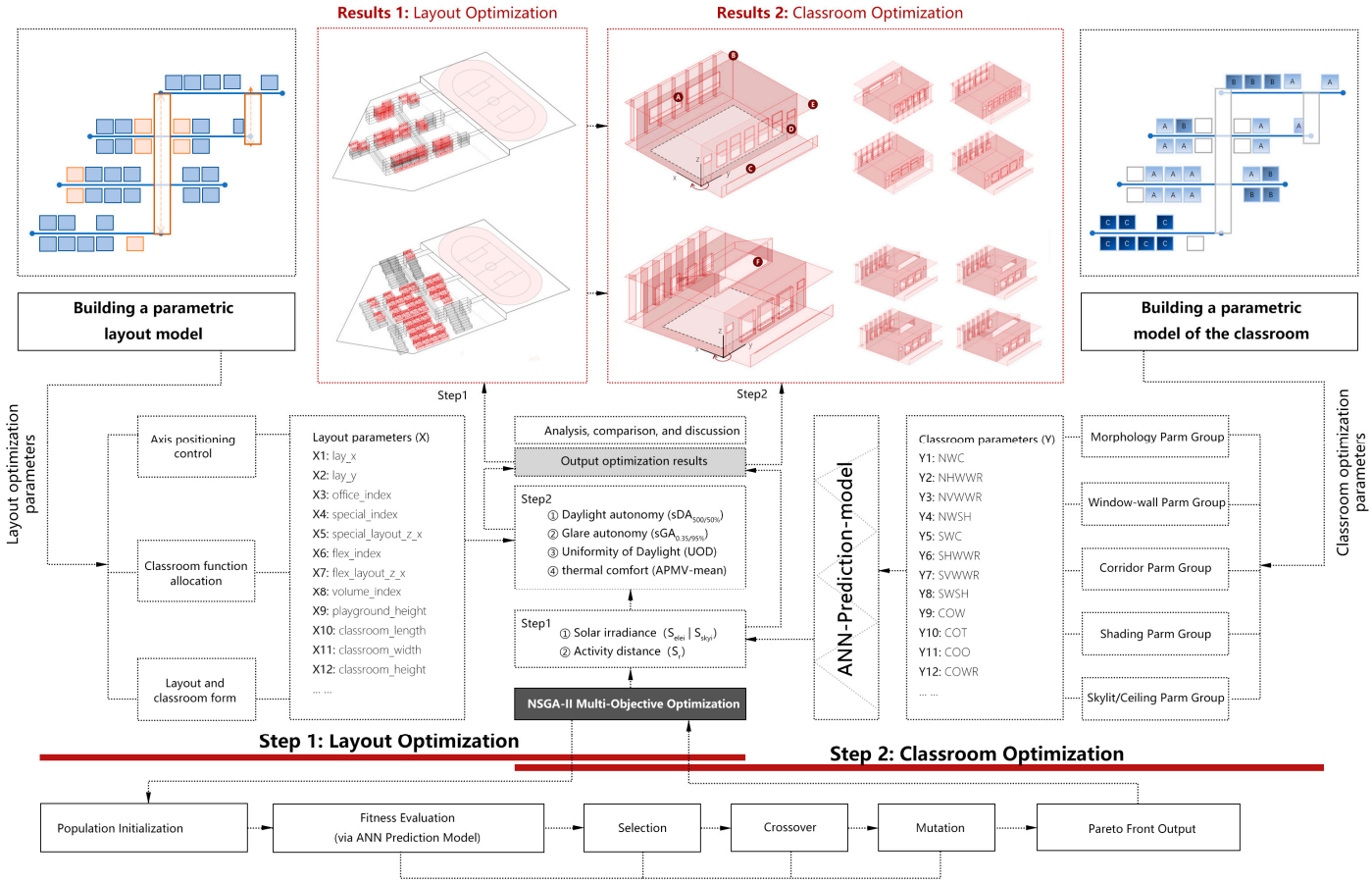


Figure 3. Research Workflow.

- **Stage 1: Layout Optimization**

This stage selects solar radiation illuminance and activity accessibility distance as evaluation indicators. These indicators are used to optimize the location and functional layout of teaching buildings, thereby determining the preliminary arrangement of classrooms.

- **Stage 2: Classroom Optimization**

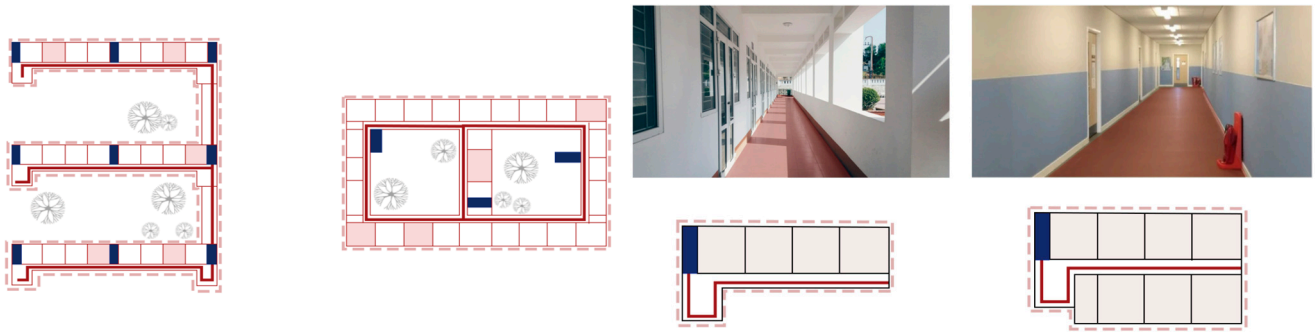
This stage is conducted based on the established overall layout. It further refines the design by optimizing classroom construction parameters, with evaluation indicators including sDA, sGA, UOD, and APMV-mean, to enhance daylighting and thermal comfort performance.

3.2. Prototypes

To establish a baseline layout and classroom prototype suitable for parametric generative research, this study combines an empirical survey with an analysis of established precedents to determine an optimal architectural configuration.

3.2.1. Layout Prototype

Two primary organizational models for school buildings were evaluated: linear matrix (Figure 4a) and courtyard layout (Figure 4b). The linear matrix layout connects functional units along a corridor, offering clear circulation, a regular structure, and a highly modular logic for construction. In contrast, the courtyard layout arranges buildings to enclose an internal court, creating rich spaces for interaction but at the risk of self-shading and less efficient circulation paths.



(**a**) (**b**) (**c**) (**d**)

Figure 4. Prototype comparison: (**a**) linear matrix layout; (**b**) courtyard layout; (**c**) single-loaded corridor; (**d**) double-loaded corridor.

To investigate the practical application of these layouts, a survey of 28 primary and secondary schools in the high-density urban contexts of Guangzhou and Shenzhen was conducted (Appendix A). The analysis revealed that:

Linear matrix and hybrid layouts are dominant (accounting for 71% of cases), especially in recently constructed, large-scale schools where their scalability and flexibility are highly valued. Courtyard layouts (29%) are more frequently found on constrained, older urban sites. Their typically higher Floor Area Ratio suggests the courtyard is often a design strategy adopted in response to dense site conditions.

Overall, the linear matrix layout demonstrates greater resilience in accommodating diverse school sizes. Its regular topology is more conducive to systematic optimization, making it a superior framework for a generative design process.

3.2.2. Corridor Prototype

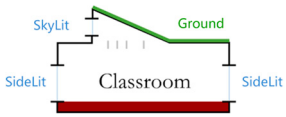
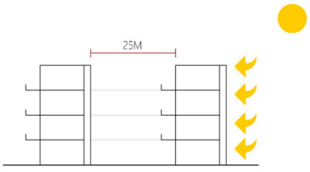
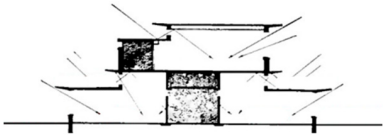
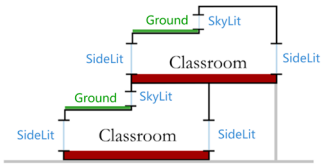
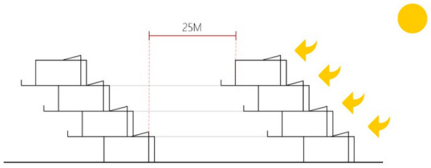
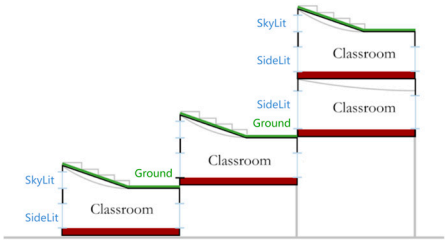
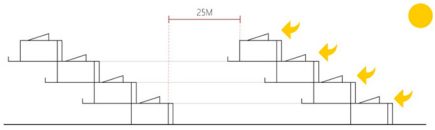
Within the linear layout, two common corridor arrangements exist: single-loaded (Figure 4c) and double-loaded (Figure 4d). A single-loaded corridor, which places classrooms along one side of an open-air walkway, ensures that all teaching spaces have direct access to natural light and cross-ventilation, leading to superior indoor environmental quality. A double-loaded corridor, while more space-efficient, inherently compromises performance by forcing one bank of classrooms to face an internal hallway, significantly limiting their access to daylight and fresh air.

This distinction is particularly critical for this study's context in the Lingnan region, where the hot and humid climate places high demands on natural ventilation and solar control. The single-loaded corridor maximizes the potential for passive environmental regulation, making it the ideal choice for this climate.

3.2.3. Classroom Prototype

These European and American schools often depend on low-rise buildings, making them less applicable to China's high-density, multi-story campuses. To address this, our team adopted a "stepped terrace" design in the construction of Kaiyuan School in Guangzhou. This design reserved skylight openings on each floor while allowing the roof slab of each classroom to serve as an outdoor platform for the upper level. In this way, the design ensured high-quality indoor daylighting while expanding students' opportunities for sunlight exposure, embodying the concept of the "Daylighting School" (Table 4).

Table 4. Insights from "Daylight Classrooms"—Prototype Extraction of the Stepped-Terrace Classroom Design (① Smith Middle School; ② North Guilford Middle School; ③ Kaiyuan School) [32,33].

	Teaching Building Layout Typology	Classroom Prototype Extraction (Section)	Sectional Morphologies of "Stepped-Terrace" Layouts
①			
②			
③			

However, a few individual "Daylighting School" cases cannot fully represent the diversity and complexity of school building types in China. Classrooms vary widely in scale and daylighting conditions, making it difficult to establish a unified framework for evaluation and design. As shown in the right column of Table 4, drawing on practical experience, this study classifies classrooms into three prototypical design models based on sectional configuration and terrace setback distance (1, 1/2, 0). These prototypes abstract diverse building forms into controllable and quantifiable models, enabling systematic analysis and parametric optimization. By distilling key spatial and geometric features, the prototypes not only reveal how different spatial configurations influence daylighting performance but also provide a generalizable and scalable framework for daylight-oriented campus design in high-density urban environments.

Therefore, based on its suitability for generative workflows, scalability, and superior environmental performance in the target climate, the linear single-loaded corridor layout is selected as the fundamental prototype for subsequent parametric modeling and performance optimization. Three classroom layout types—*Standard Side-Lit Classroom* (control group), *High Side-Lit Classroom* and *Skylight-Lit Classroom* (experimental group)—were used as generative prototypes, each producing multiple optimized schemes for selection and comparison. The study employed Rhino 7 (SR33) & Grasshopper 1.0.0007 (Wallacei V2.7) [54] for generative optimization and visualization, while integrating the hops [55] plugin with the Visual Studio Code (V1.101.2)—Python (V3.8.12) platform to enable real-time prediction of the four daylighting and thermal indicators during the optimization process.

3.3. Experimental Site

Guangzhou serves as a representative case for studying climate-responsive design in the Lingnan region, due to its typical subtropical monsoon climate. The city's education sector is also expanding rapidly, adding 319,200 student places in the last three years, the highest growth in the region [56]. This immense demand for new school facilities places significant pressure on architectural quality and performance, making Guangzhou

an ideal testing ground for innovative design methodologies. This study selected a planned educational reserve site in Guangzhou as the experimental location (Figure 5).



Figure 5. Site selection for teaching area generation experiment (site indicates generation boundary).

The site is adjacent to major urban roads on the south and east sides, providing convenient transportation. The north side is reserved for supporting facilities such as canteens and administrative offices. Due to proximity to an expressway and associated noise, a standard elevated playground was arranged on the east side. In the experiment, the shortest access path for students was calculated to optimize the elevation height. The southwest portion serves as the core teaching cluster, which is the generation and optimization target of the "Sunshine School" classroom complex. The site is an irregular polygon with complex boundaries, making it suitable for testing the algorithm's geometric adaptability and robustness under non-standard land conditions.

3.4. Stage 1: Layout Models

3.4.1. Layout Parametric Models

The layout model adopts the "linear matrix corridor layout" as the core generative framework. By integrating the designated site boundary and the current design codes, a set of parametric design rules based on functional distribution is established. Ordinary classrooms, flexible classrooms, specialized classrooms, and faculty offices are interlaced, while building positions and setbacks are fine-tuned through volumetric displacement and rooftop combinations to explore optimal arrangements.

The layout rules are divided into two categories: fixed parameters, determined by mandatory Chinese design codes, and rule-based parameters, defined by functional allocation and diversification strategies within specified ranges (Table 5).

Table 5. Layout Rule Parameters.

Controlled form	Variable Name	Abbreviation	Value Range	Step Size	Number of Values
Function Distribution Ratio	School scale: Ordinary classroom: Flexible classroom: Special classroom: Teacher's office	S:O:F:S:T	24:24:6:6:6 30:30:8:8:8 36:36:9:9:9 48:48:12:12:12 60:60:15:15:15	-	5
Layout Parameters					
North–South Axial Positioning Control	lay_x	LX	0~1	1	2
East–West Axial Positioning Control	lay_y	LY	0~4	1	5
Office Layout Enumeration	office_index	OI	0~10	1	11
Specialized Classroom Layout Enumeration	special_index	SI	0~20	1	21
Specialized Classroom Layout Typology	special_layout_z_x	SLZX	0~1	1	2
Flexible Classroom Layout Enumeration	flex_index	FI	0~20	1	21
Flexible Classroom Layout Typology	flex_layout_z_x	FLZX	0~1	1	2
Subtracted Volume Enumeration	volume_index	VI	0~20	1	21
Raised Height of Playground (Activity Space)	Playground_height	PH	0~8 m	0.5 m	17
Form Parameters					
Classroom Length	classroom_length	CL	8.4~10.8 m	0.6 m	5
Classroom Width	classroom_width	CW	7.2~9.6 m	0.6 m	5
Classroom Height	classroom_height	CH	3.6~4.8 m	0.3 m	5

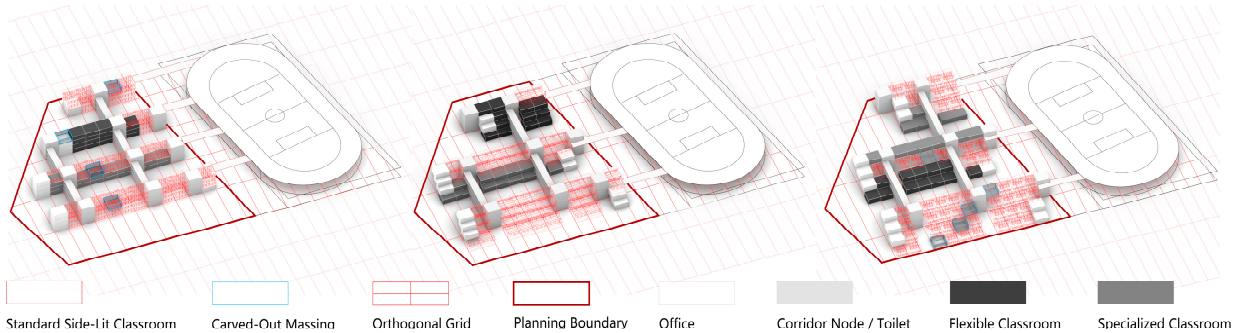
The generative logic includes:

- Building boundary input: Functional zones are delineated according to the site boundary, with playgrounds reserved. A setback of one classroom length (CL) is maintained on all sides as the construction limit, forming a grid system that ensures compliance with spacing requirements.
- Initial nodes and egress system: Centered on the corridor origin, egress nodes (circulation cores and restrooms) are generated through a fixed-step array, with automatic rule checking to supplement staircases at corridor ends.
- Axis adaptive adjustment: A dual-parameter control model (1/2 span adjustment in the north–south direction, 1/5 span adjustment in the east–west direction) is introduced to accommodate coordinate shifts, balancing layout diversity with regulatory compliance.
- Functional space allocation: The total number of classrooms is calculated based on the school scale. Surplus grid nodes are treated as "void volumes" to enhance morphological diversity. Offices are allocated first, followed by specialized and flexible classrooms arranged according to vertical/horizontal stratification, while the remaining nodes are automatically assigned as ordinary classrooms.

$$N_{grid} = N_{void} + \left(N_{office} + N_{ordinary} + N_{flex} + N_{special}\right) \quad (1)$$

In Equation (1), N_{grid} denotes the total number of initialized grid nodes, N_{void} the number of void volumes, N_{office} the number of offices, $N_{ordinary}$ the number of ordinary classrooms, $N_{special}$ the number of specialized classrooms, and N_{flex} the number of flexible classrooms.

As shown in Figure 6, the parametric campus layout generation system, developed on Rhino and Grasshopper, achieves intelligent configuration of the architectural skeleton under regulatory constraint algorithms.



(**a**) (**b**) (**c**)

Figure 6. Illustration of parametric layout design based on functional allocation: (**a**) Standard Side-Lit Classroom, (**b**) High Side-Lit Classroom, (**c**) Skylight-Lit Classroom.

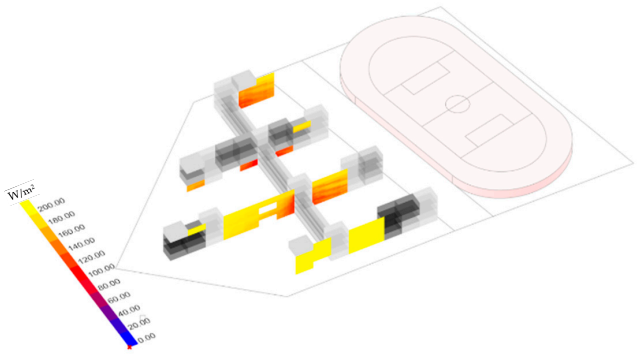
3.4.2. Layout Evaluation Indicators

- **Solar Irradiance:** Maximizing Site Daylighting Potential

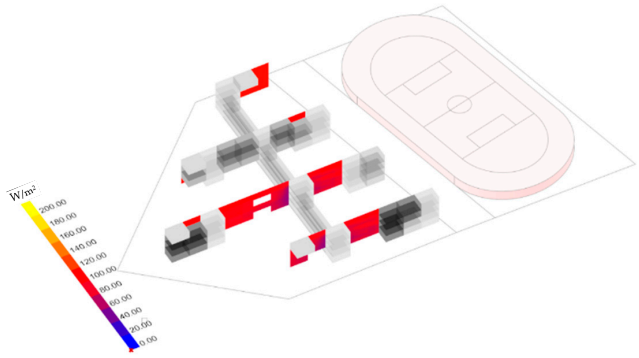
During the generation of teaching building layouts, the foremost consideration is the daylighting condition of the site. The solar irradiance on the north–south façades and skylights of standard classrooms is measured to preliminarily assess the adequacy of daylighting under the current spatial arrangement of the classroom cluster. This provides the basis for subsequent evaluation of indoor daylighting performance (Figure 7).

$$S_{elei} = \frac{S_{North-ir} \times S_N + S_{South-ir} \times S_S}{S_N + S_S} \quad (2)$$

$$S_{skyi} = S_{sky-ir} \quad (3)$$



(**a**)



(**b**)

Figure 7. Visualization of (standard side-lit classroom layout example): (**a**) South Façade, (**b**) North Façade.

In Equations (2) and (3), S_{elei} denotes the solar irradiance received by the classroom façades, $S_{South-ir}$ and $S_{North-ir}$ represent the solar irradiance on the south and north façades, S_N and S_S are the corresponding façade areas, and S_{sky-ir} is the solar irradiance received by skylight roofs.

- **Activity Accessibility Distance:** Optimizing Inter-Class "Chasing Daylight" Routes

To quantify students' accessibility from classrooms to outdoor activity spaces during class breaks, the study referred to the national compulsory education curriculum schedule and collected timetables from nine high schools in Guangdong [57–60]. First, the time allocation of core compulsory subjects, elective modules, and arts/physical education courses was analyzed. Second, spatiotemporal usage patterns of three classroom types (ordinary, flexible, and specialized) were recorded through online community surveys (Table 6). Finally, to abstract the probability distribution of students moving from different classroom types to outdoor activities, the study introduced activity accessibility distance (Figure 8) as a key indicator, with weighting based on the classroom person–time utilization rate (r_{s-t}), thereby integrating it into the evaluation framework for design optimization.

$$S_r = D_{ds1\to pg} + D_{dsn\to ds1} + D_{cls\to ds} \tag{4}$$

Table 6. The median values of the samples were extracted to calculate the person–time utilization rates for the experimental indicators.

Classroom Type	Ordinary	Flexible	Specialized
Utilization Rate (%)	60.44	28.20	11.36

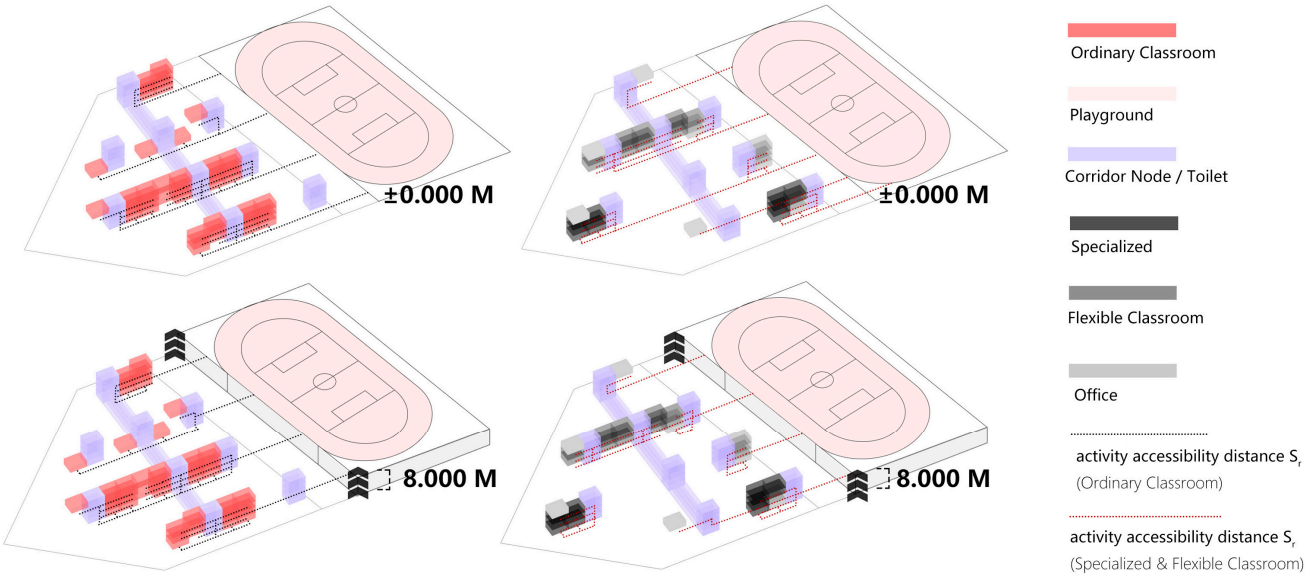


Figure 8. 0 M/8 M Playground Height: activity accessibility distance $\overline{S}_r$ (e.g., Standard Side-Lit Classroom layout).

In Equation (4), $D_{cls\to ds}$ denotes the evacuation distance from the classroom to the nearest staircase, $D_{dsn\to ds1}$ the distance from the staircase to the evacuation floor (aligned with the playground if elevated), and $D_{ds1\to pg}$ the distance from the evacuation floor to the playground. The activity accessibility distance S_r of a single classroom is thus the sum of the three components.

$$\overline{S}_r = \frac{\sum_{i=0,type\in\{\text{ordinary,flexible,specialized}\}}^{n} r_{s-t,i,type} \cdot S_{r,i,type}}{n} \tag{5}$$

In Equation (5), $r_{s-t,i,\ type}$ is the person–time utilization rate of a given classroom type, and $S_{r,i,type}$ is its corresponding accessibility distance. The weighted mean accessibility distance $\overline{S}_r$ thus represents the cluster-wide accessibility performance, accounting for differentiated classroom utilization patterns.

3.5. Stage 2: Classroom Clusters Models

3.5.1. Classroom Parametric Models

After completing the layout model, the study selected ordinary classrooms—characterized by the longest average student learning time, the strictest daylighting requirements, and the highest utilization rate—as the focus for developing a parametric interior model.

The model enables geometry to be updated in real time through parameter-driven transformations, allowing adaptive adjustments of spatial form to achieve precise control of natural daylight performance (Table 7). Based on a typological approach, the design variables are organized into six parameter groups: form, window-wall, corridor, shading, skylight, and ceiling (Figure 9). Among these, skylight parameter group applies only to the High Side-Lit Classroom and the Skylight-Lit Classroom, and ceiling parameter group is exclusive to the Standard Side-Lit Classroom. The remaining four parameter groups are shared across all classroom types.

Table 7. Rule parameters for classroom design (Application classrooms: ①—Standard side-lit classroom, ②—High side-lit classroom, ③—Skylight-lit classroom).

Variable Name	Abbreviation	Value Range	Step Size	No. of Values	Application Classroom
Morphological parameters					
classroom_length	CL	8.4~10.8 m	0.6 m	5	All
classroom_width	CW	7.2 ~9.6 m	0.6 m	5	All
classroom_height	CH	3.6~4.8 m	0.3 m	5	All
wall_pillar_width_with_door	WPWD	0.9~2.1 m	0.6 m	3	All
wall_pillar_width_without_door	WPWOD	0.6~1.2 m	0.6 m	2	All
Window-wall parameters					
north_window_count	NWC	1~6	1	6	All
north_horizontal_window_wall_ratio	NHWWR	0.4~0.9	0.1	6	All
north_vertical_window_wall_ratio	NVWWR	0.4~0.9	0.1	6	All
north_window_frame_thickness	NWFT	0.1~0.5 m	0.1 m	5	All
north_window_sill_height	NWSH	0.3~1.0	0.1	8	All
north_inner_window_frame_height	NIWFH	0.2~0.8	0.2	4	All
south_window_count	SWC	1~6	1	6	All
south_horizontal_window_wall_ratio	SHWWR	0.4~0.9	0.1	6	All
south_vertical_window_wall_ratio	SVWWR	0.4~0.9	0.1	6	All
south_window_frame_thickness	SWFT	0.1~0.3 m	0.1 m	3	All
south_window_sill_height	SWSH	0.3~1.0	0.1	8	All
south_inner_window_frame_height	SIWFH	0.2~0.8	0.2	4	All
Corridor parameters					
corridor_width	COW	2.1~3.0 m	0.3 m	4	All
corridor_type	COT	0~2	1	3	All
corridor_orientation	COO	0~1	1	2	①③
corridor_window_ratio	COWR	3~6	1	5	All
ventilated_window_height	VWH	0.3~0.9 m	0.3 m	3	All

Table 7. *Cont.*

Variable Name	Abbreviation	Value Range	Step Size	No. of Values	Application Classroom
Shading parameters					
shading_width	SW	0.3~1.8 m	0.3 m	6	All
vertical_blind_count	VBC	2~8	2	4	All
vertical_blind_width	VBW	0~0.8 m	0.2 m	5	All
vertical_blind_rotation_angle	VBRA	−60~90°	30°	6	All
Skylight/Ceiling parameters					
skylight_height	SH	0.6~2.4 m	0.6 m	4	②③
parapet_height	PH	0.1~0.5 m	0.2 m	2	③
south_setback	SS	0.6~2.4 m	0.6 m	4	③
north_setback	NS	3.0~4.2 m	0.6 m	2	③
east_setback	ES	0.6~3.0 m	0.6 m	4	③
west_setback	WS	0.6~3.0 m	0.6 m	4	③
skylight_angle	SA	0~4	1	5	③
skylight_grille_count	SGC	2~8	2	4	②③
skylight_grille_thickness	SGT	0~0.3 m	0.1 m	4	②③
ceiling_grille_count	CGC	2~8	2	4	②③
ceiling_grille_thickness	CGT	0~0.3 m	0.1 m	4	②③
ceiling_foldline_position_factor	CFPF	0~0.8	0.2	5	①②
ceiling_tilt_height	CTH	0~0.9 m	0.3 m	4	①②

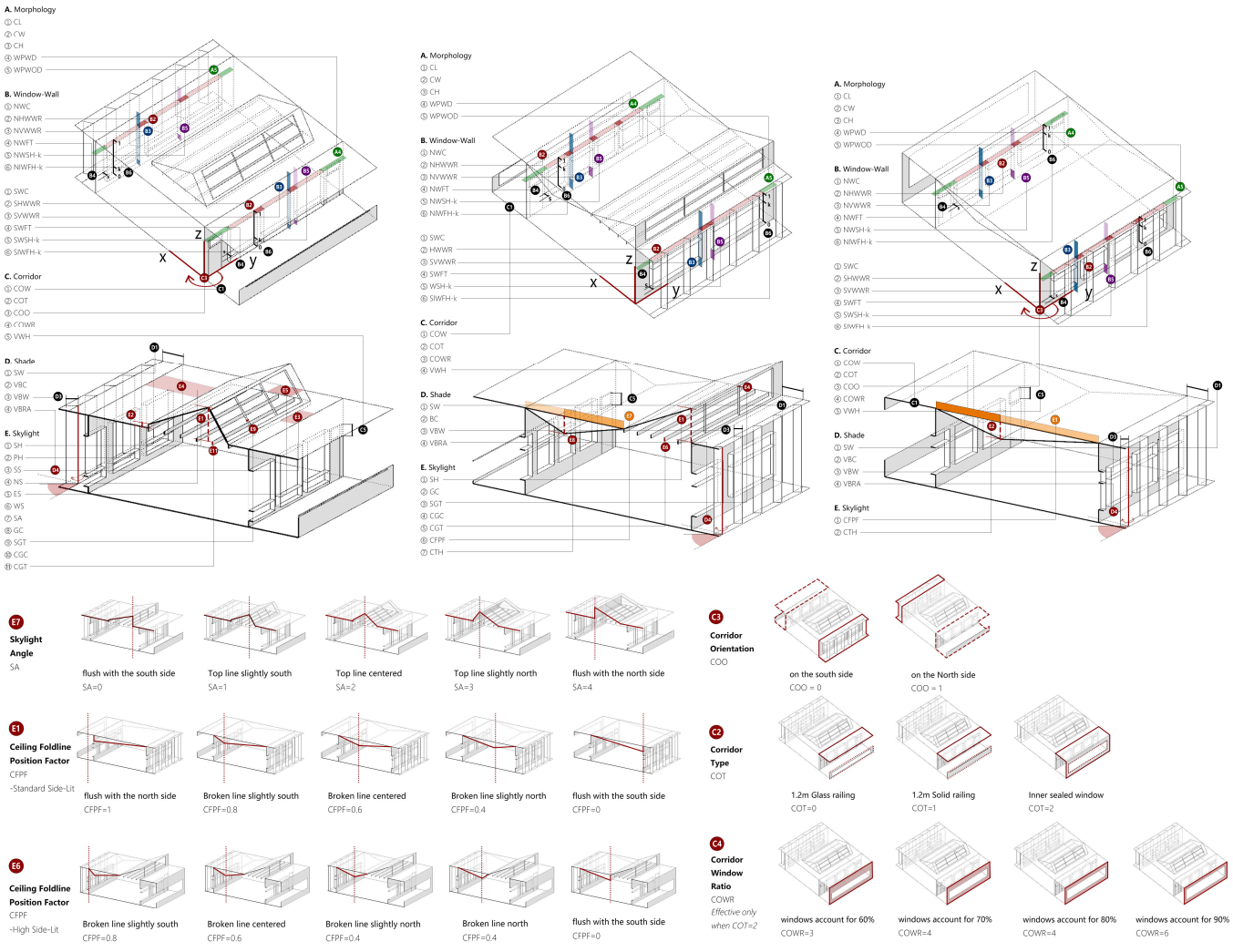


Figure 9. Design parameter breakdown of three classroom types.

3.5.2. Classroom Evaluation Indicators

In light of the daylight climate characteristics of southern China, Liu et al. [61], based on field measurements and questionnaire surveys conducted in 18 classrooms at a high school in Guangzhou, found that $sDA_{500lx/50\%}$ is highly correlated with daylight satisfaction, while $sGA_{0.35/95\%}$ shows a significant correlation with glare perception. This approach proves to be more effective than directly applying the highest standards of the European Union. The recommended thresholds are not only higher than the 450 lx requirement stipulated in the General Code for Building Environment [62] for primary and secondary school classrooms in China, but also consistent with the upper limits of visual comfort defined in EN17037 [63] and IES [64] standards, and significantly superior to those adopted in North America and by USGBC [65].

Accordingly, this study adopts $sDA_{500lx/50\%}$, $sGA_{0.35/95\%}$, UOD, and APMV-mean as the four evaluation indicators for constructing a multi-objective optimization framework for classroom clusters. Among them, sDA measures daylight sufficiency, sGA evaluates glare risk, UOD reflects daylight uniformity, and APMV-mean controls thermal discomfort caused by excessive solar gains (Table 8).

Table 8. Design-oriented optimization objectives of classroom parameters.

Indicator	Recommended Value	Definition	Reference
Spatial Daylight Autonomy ($sDA_{500lx/50\%}$)	$\geq$0.5	Proportion of floor area where illuminance exceeds 500 lx for more than 50% of the occupied time under natural daylight conditions.	Liu et al. [61]
Spatial Glare Autonomy ($sGA_{0.35/95\%}$)	$\geq$0.5	Percentage of viewpoints at 0.7 m above the floor level where the Daylight Glare Probability (DGP) is less than 0.35 for 95% of the year, indicating compliance with glare comfort standards.	Liu et al. [61]
Uniformity of Daylight (UOD)	$\geq$0.5	Ratio of minimum illuminance to average illuminance, representing the uniformity of light levels across different positions or areas.	Evaluation Standard for Indoor Thermal and Humidity Environment of Civil Buildings (GB/T 50785-2023) [66]
Adaptive Predicted Mean Vote (Mean) APMV-mean	$\lvert value \rvert \leq 1$	Predicts overall human thermal sensation by comprehensively considering indoor environmental factors (air temperature, relative humidity, air speed, external environmental conditions) and human factors (metabolic rate, clothing, activity level, etc.).	General Code for Building Environment (GB 55016-2021) [62]

3.6. Development of Two-Stage Generative Platform

As shown in Figure 10, after completing the two parametric modeling components, a GA–ANN-based simulation–prediction–optimization platform was established. First, performance models of sample classrooms were built using Rhino and Grasshopper, with Ladybug (V1.6.0) and Honeybee (V1.6.0) serving as the simulation interfaces. Subsequently, performance simulations were conducted through Honeybee and EnergyPlus (V1.6.0) for four key indicators, generating a large-scale dataset. The dataset was then analyzed to assess the correlation between classroom parameters and performance metrics, eliminating irrelevant variables and reducing dimensionality to lower prediction complexity. After constructing the ANN prediction model, the optimized parameter sets were divided into

training, testing, and validation subsets, followed by hyperparameter tuning to ensure minimal training loss. The finalized ANN model was trained with the dataset and subsequently evaluated for its fitting accuracy and predictive reliability.

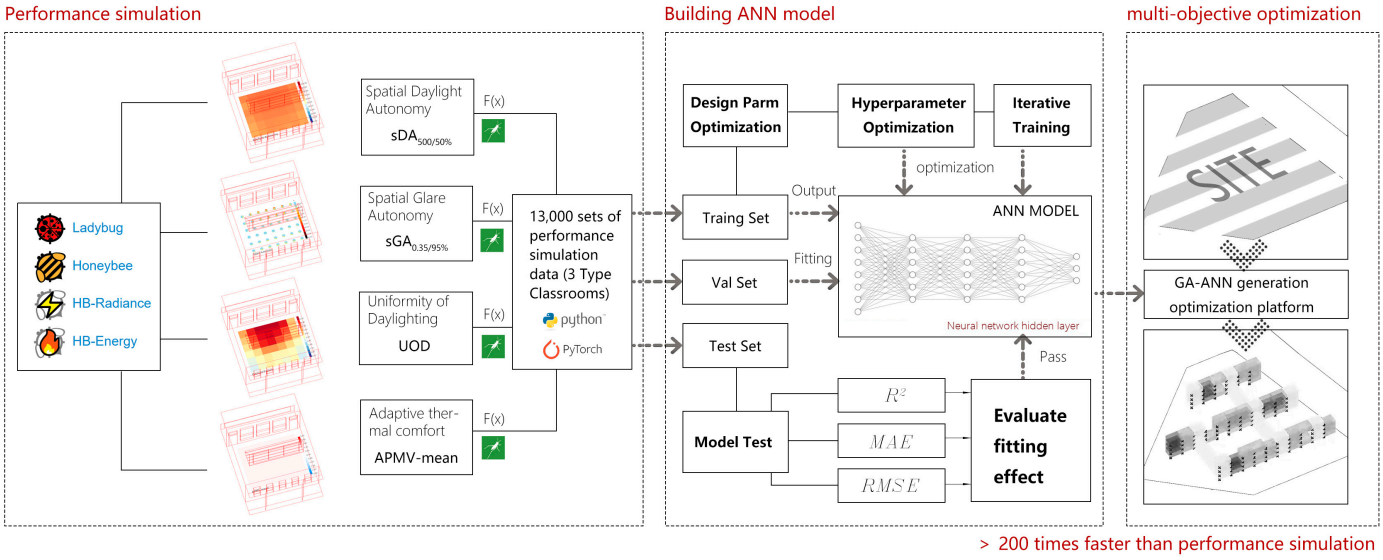


Figure 10. ANN prediction model training framework for classroom clusters.

Once validated, the ANN model was integrated into the Stage 2 classroom optimization process to accelerate performance evaluation. Because the parameter dependencies differ among the three daylighting strategies—standard side-lit, high side-lit, and skylight-lit classrooms—independent prediction models were trained for each, with their predictive performance analyzed separately in subsequent evaluations.

3.6.1. Performance Simulation

For dataset construction, parametric classroom models were established in Rhino & Grasshopper. Key settings include a 0.7 m working plane, 0.5 m × 0.5 m grid resolution, and a UOD evaluation domain reduced by 1 m on each side to exclude blackboard and corridor areas. The climate input was based on Guangzhou Typical Meteorological Year (TMY), with a simulation period covering 8 school months (excluding summer/winter vacations and weekends), from 8:00–12:00 and 14:00–17:00 daily, consistent with daylighting simulation schedules to ensure realistic usage conditions. Performance samples were generated in batches using Ladybug, Honeybee, and EnergyPlus. Simulation parameters were set as follows:

- **Optical properties:** Interior surfaces finished with super-white mineral-based coating ($\rho = 0.75$), light-colored terrazzo flooring ($\rho = 0.50$), wood–plastic decking for exterior corridors ($\rho = 0.35$), aluminum shading devices ($\rho = 0.85$), and double-glazed low-E windows with aluminum frames ($\tau = 0.60$).
- **Thermal properties:** Envelope heat transfer coefficients: roof $K \leq 0.40$ W/(m^2·K), exterior wall $K = 0.31$ W/(m^2·K), low-E double glazing $K = 1.80$ W/(m^2·K), SHGC = 0.35, $\tau = 0.60$. Indoor loads: occupant density 1.66 m^2/person, equipment load 15 W/m^2, and metabolic heat gain 140 W/person.

3.6.2. Building ANN Model

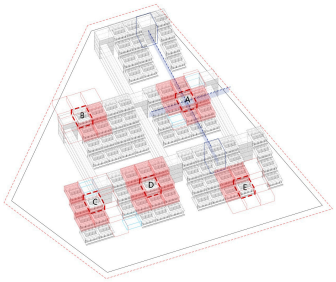
To address the high computational cost and inefficiency of traditional simulation engines in optimizing high-density classroom clusters, this study developed an **Artificial Neural Network (ANN) prediction model** (Figure 10). The model enables fast prediction of daylighting and thermal performance indicators, providing an efficient tool for subsequent

multi-objective optimization. The ANN is designed as a multi-layer feedforward network with fully connected layers, consisting of input, hidden, and output layers. Training involves forward propagation, where sample data are transmitted layer by layer to generate predictions, followed by backpropagation, where gradients of the loss function with respect to weights are computed via the chain rule and optimized iteratively using the Adam optimizer to minimize errors.

After simulation, correlation analysis was conducted between design parameters and performance metrics to remove redundant variables and reduce prediction complexity. Hyperparameters [67] were optimized using **Bayesian Optimization (BO)** [68], which identifies optimal ANN configurations by constructing probability distributions of the objective function and applying the Expected Improvement criterion. The trained ANN model was then quantitatively evaluated through fitting accuracy and error indicators.

It is worth noting that most existing classroom daylighting studies assume unobstructed external conditions, ignoring the significant impact of building height and mutual shading within teaching clusters. Daylight and solar radiation vary substantially across floors and positions. As shown in Table 9, this study introduces two cluster correction parameters into the ANN model:

Table 9. Environmental correction parameters of classroom clusters: 5 target classrooms (A–E).

		A	**B**	**C**	**D**	**E**
	R_p	$\begin{bmatrix}1&1&0\\1&3&1\\0&1&1\end{bmatrix}$	$\begin{bmatrix}0&0&0\\0&4&1\\0&1&1\end{bmatrix}$	$\begin{bmatrix}1&0&0\\1&3&0\\1&1&0\end{bmatrix}$	$\begin{bmatrix}1&1&1\\1&3&1\\1&1&1\end{bmatrix}$	$\begin{bmatrix}1&1&0\\1&1&0\\0&0&0\end{bmatrix}$
	R_e	$\begin{bmatrix}1\\0\\1\end{bmatrix}$	$\begin{bmatrix}0\\-1\\1\end{bmatrix}$	$\begin{bmatrix}0\\1\\0\end{bmatrix}$	$\begin{bmatrix}1\\0\\0\end{bmatrix}$	$\begin{bmatrix}1\\1\\0\end{bmatrix}$

- Relative Position Parameter (R_p): Captures the target classroom's floor level and adjacency relations (0/1) with surrounding classrooms (above, below, west, east), floor number (1–4).

$$R_p = \begin{Bmatrix} West\ above\ [0,1] & Above\ [0,1] & East\ above\ [0,1] \\ West\ [0,1] & Floor\ level\ [1,4] & East\ [0,1] \\ West\ below\ [0,1] & Below\ [0,1] & East\ below\ [0,1] \end{Bmatrix}$$

- Layout Environment Parameter (R_e): Reflects the presence of north–south obstructions and east–west corridors. Obstructions are described as binary (0/1), while corridor conditions are expressed as $-1/0/1$.

$$R_e = \begin{Bmatrix} North\ obstruction\ [0,1] \\ East-west\ corridor\ [-1,0,1] \\ South\ obstruction\ [0,1] \end{Bmatrix}$$

3.6.3. Genetic Algorithm Multi-Objective Optimization

NSGA-II [69] (Non-dominated Sorting Genetic Algorithm II) is a multi-objective evolutionary algorithm based on fast non-dominated sorting, crowding distance comparison operator, and elitist preservation strategy. It can efficiently approximate the Pareto optimal solution set while maintaining population diversity. In this study, the NSGA-II algorithm

was adopted as the optimization model, and the two stages of multi-objective optimization were formulated as follows:

- Stage 1: Layout optimization

$$S_1 = F(x)_{min}\left[S_r(x); -S_{elei}(x); -S_{skyi}(x)\right] \quad (6)$$

- Stage 2: Classroom optimization

$$S_2 = F(x)_{min}[-S_{uod}(x); -S_{sDA}(x); -S_{sGA}(x); S_{APMV}(x)] \quad (7)$$

In Equations (6) and (7), S_1 and S_2 represent the multi-objective optimization scores, while x denotes the iteration number. Since Pareto optimization requires minimization of objective functions, the solar radiation scores $S_{elei}(x)$ and $S_{skyi}(x)$, as well as daylighting indices including uniformity of daylighting $S_{uod}(x)$, spatial daylight autonomy $S_{sDA}(x)$, and spatial glare autonomy $S_{sGA}(x)$ are all taken as negative values, In contrast, activity accessibility $S_r(x)$ and adaptive thermal comfort $S_{APMV}(x)$ are kept as their original values.

To realize daylighting optimization for different classroom types, specific parameter configurations were set according to the two optimization stages, as shown in Table 10.

Table 10. Multi-objective optimization parameter settings.

Optimization Step	**Step1: Layout Optimization**			**Step2: Classroom Optimization**		
Type	Standard Side-Lit	High Side-Lit	Skylight-Lit	Standard Side-Lit	High Side-Lit	Skylight-Lit
Generation Size	40	40	40	40	40	40
Generation Count	40	40	40	40	40	40
Crossover Probability	0.9	0.85	0.85	0.9	0.85	0.85
Mutation Probability	1/0.9	1/0.85	1/0.85	1/0.9	1/0.85	1/0.85
Crossover Distribution Index	20	20	20	20	20	20
Mutation Distribution Index	20	20	20	20	20	20
Number of Genes	11	11	11	20	22	26
Number of Values	101	101	101	119	135	135
Number of Fitness Objectives	2	3	3	4	4	4
Size of Search Space	6.1×10^8	6.1×10^8	6.1×10^8	6.4×10^{15}	2.6×10^{16}	1.8×10^{18}

4. Result

4.1. Dataset Processing

During dataset preparation, three classroom models were built in Grasshopper. Boolean switches were used to control structural types (e.g., skylights, corridor forms), while sliders dynamically adjusted over 20 design parameters, including classroom length, width, height, skylight offset angle, and window-to-wall ratio, enabling 3D visualization and type linkage. Sample generation was conducted using the Anemone plugin to construct nested loops, combined with Python scripts (V2.7.12) and Parallel Loops (Anemone V0.4 for Grasshopper) for multi-machine parallel computing, with computation states recorded in JSON files.

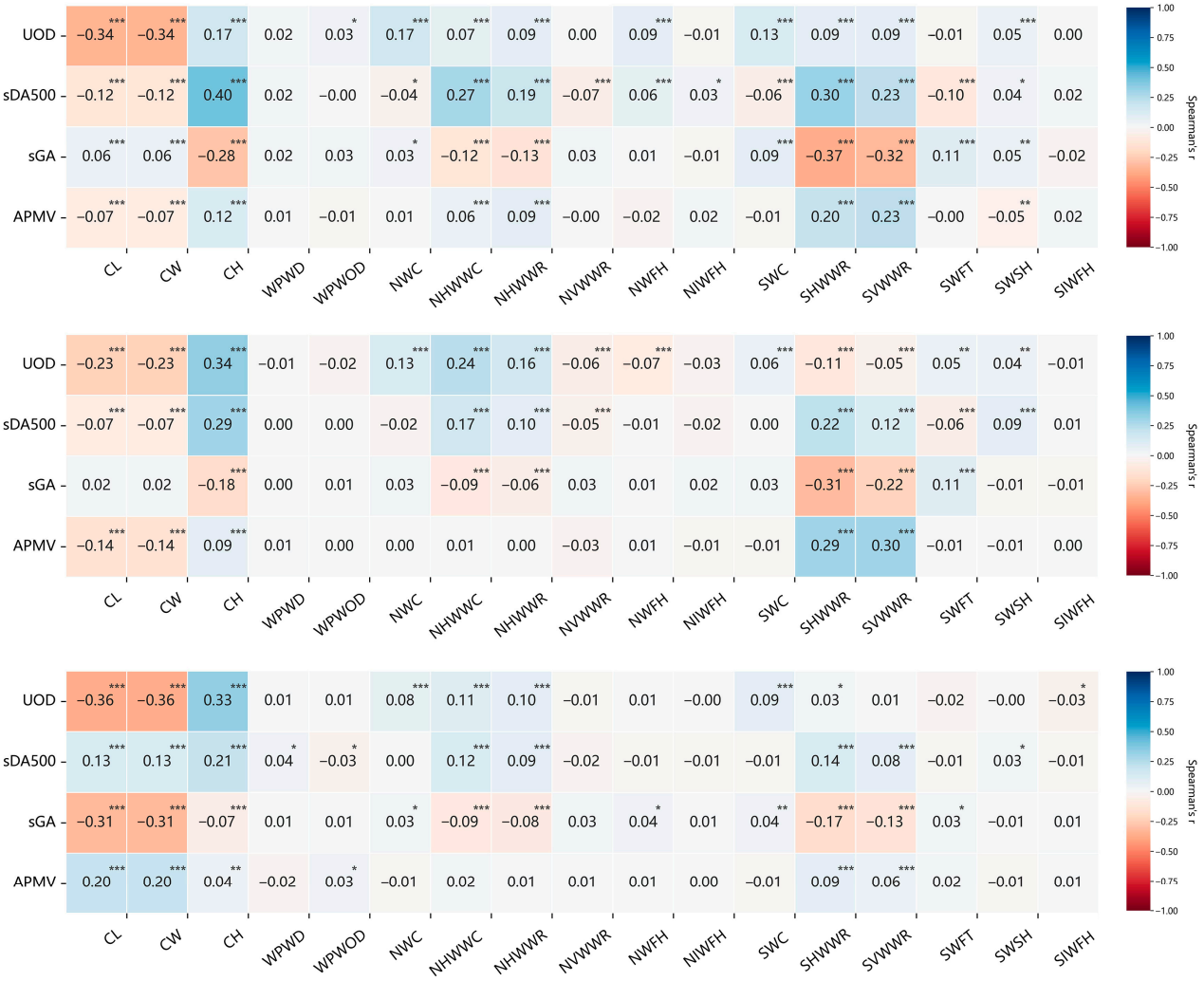
The experiments were conducted on a computer (R7-5700X CPU, 32 GB RAM, 1070 Ti GPU). Each sample required approximately 2 min and 15 s on average, with a total runtime of 486 h 40 min. A total of 14,320 samples were generated, of which 13,000 remained after cleaning (5000 skylight, 4000 high side window, 4000 conventional side window). During ANN model training, data were stratified by classroom type and randomly divided into training and test sets in an 8:2 ratio, stored in CSV format. The distribution of design variables across the samples was relatively uniform and approximately linear, ensuring data continuity and generalizability for model training.

To further refine input variables, Spearman's rank correlation coefficient (ρ) [70] was employed to quantify monotonic relationships between parameters and indicators, as well as among indicators themselves (Figure 11). The calculation formula is:

$$\rho = 1 - \frac{\sigma \sum d_i^2}{(n^2 - 1)} \tag{8}$$

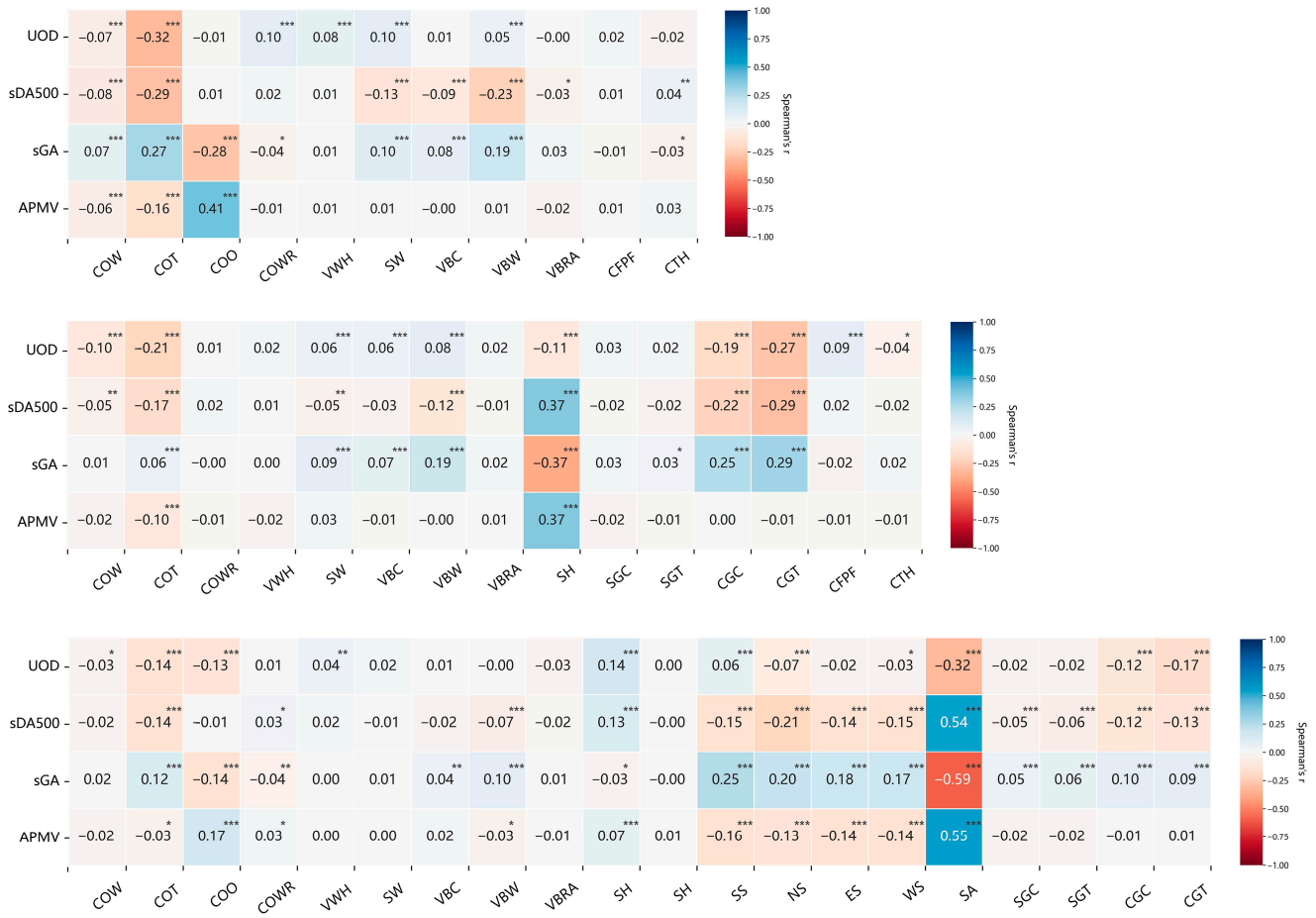
where d_i represents the rank difference and n is the sample size.

Based on the correlation analysis, parameters showing significant influence were included as model input variables, while those exhibiting weak or negligible correlations with the four performance indicators ($|\rho| \leq 0.05$) were fixed at constant values and excluded from the predictive model. After optimization, excluding environmental variables and the predetermined classroom dimensions (length, width, and height) from the layout, the number of input parameters was reduced to 17 for standard side-lit classrooms, 19 for high side-lit classrooms, and 23 for skylight-lit classrooms.



(**a**)

Figure 11. *Cont.*



(**b**)

Figure 11. (**a**,**b**) Correlation (ρ) and significance (*p*) between design parameters and performance metrics (from (**top**) to (**bottom**): standard side-lit, high side-lit, and skylight-lit classrooms). The correlation coefficient (ρ) ranges from −1 to 1; asterisks denote significance levels ($p < 0.05$ *, $p < 0.01$ **, $p < 0.001$ ***).

4.2. ANN Training Results

Since the ANN models require separate training, hyperparameter optimization was conducted individually for the datasets of the three classroom types. A Bayesian hyperparameter optimization was performed using Optuna (V3.6) [71], with 100 training epochs set as the convergence criterion for a single evaluation. Through 300 iterations, the search covered five key parameter spaces—number of hidden layers, number of neurons per layer, learning rate, batch size, and dropout rate—ultimately determining the optimal combination based on the minimum loss. The optimized hyperparameter settings, summarized in Table 11, were applied to the subsequent ANN training.

Table 11. Optimal hyperparameter combinations after Bayesian optimization.

Classroom Type	Output Feature	Batch Size	Learning Rate	Dropout	Hidden nc	N Layers	Val Loss
Standard Side-Lit Classroom	UOD	256	1×10^{-2}	0.3	128	4	0.0110
	$sDA_{500lx/50\%}$	128	1×10^{-2}	0.3	256	9	0.0096
	$sGA_{0.35/95\%}$	128	1×10^{-2}	0.2	128	4	0.0023
	APMV-mean	128	1×10^{-2}	0	128	3	0.0001

Table 11. *Cont.*

Classroom Type	Output Feature	Batch Size	Learning Rate	Dropout	Hidden nc	N Layers	Val Loss
High Side-Lit Classroom	UOD	128	1×10^{-2}	0.4	256	4	0.0058
	$sDA_{500lx/50\%}$	256	1×10^{-3}	0.2	512	9	0.0078
	$sGA_{0.35/95\%}$	128	1×10^{-2}	0.2	256	7	0.0021
	APMV-mean	64	1×10^{-2}	0.1	128	3	0.0003
Skylight-Lit Classroom	UOD	128	1×10^{-2}	0.4	256	5	0.0089
	$sDA_{500lx/50\%}$	256	1×10^{-2}	0.3	256	6	0.0093
	$sGA_{0.35/95\%}$	128	1×10^{-2}	0.3	512	5	0.0030
	APMV-mean	512	1×10^{-2}	0.2	128	3	0.0008

For model performance evaluation, four statistical indicators were employed: coefficient of determination (R^2), mean squared error (MSE), root mean squared error (RMSE), and mean absolute error (MAE). Their definitions, formulas, and evaluation thresholds are presented in Table 12.

Table 12. Explanation of evaluation metrics for the prediction model.

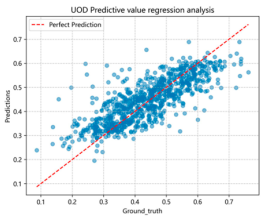
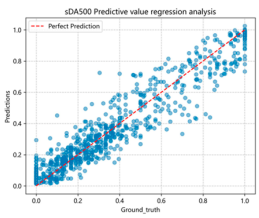
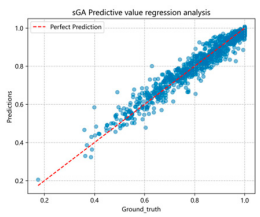
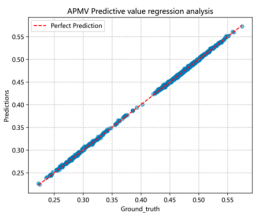
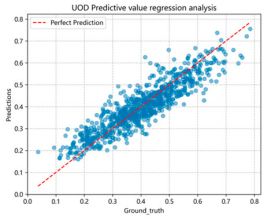
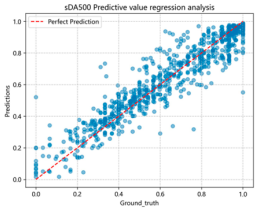
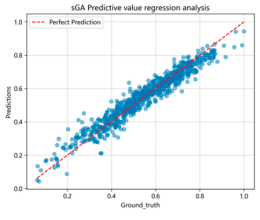
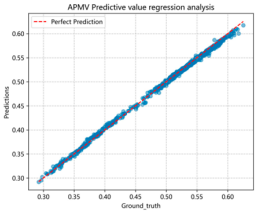
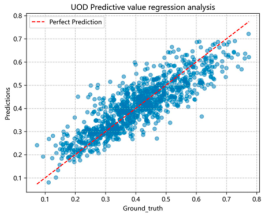
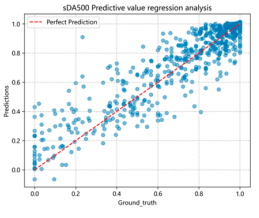
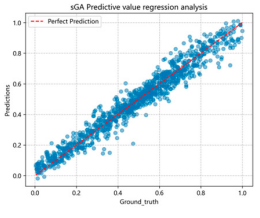
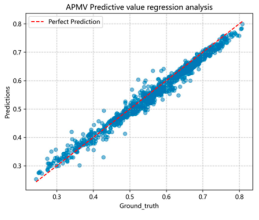
Metric	Formula	Concept
R^2	$R^2 = 1 - \frac{\sum_{i=1}^{n}(y_i - \hat{y}_i)^2}{\sum_{i=1}^{n}(y_i - \bar{y})^2}$	Quantifies how well the model explains the variance of the target variable; indicates the goodness of fit between predictions and actual values.
MSE	$MSE = \frac{1}{n}\sum_{i=1}^{n}(y_i - \hat{y}_i)^2$	Measures the average of squared prediction errors; penalizes larger errors more heavily.
RMSE	$RMSE = \sqrt{MSE}$	The square root of MSE; restores the original unit of the target variable.
MAE	$MAE = \frac{1}{n}\sum_{i=1}^{n}\lvert y_i - \hat{y}_i \rvert$	Measures the average absolute difference between predicted and actual values; reflects the typical magnitude of error.

Tables 13 and 14 show that $sGA_{0.35/95\%}$ and APMV-mean achieved the highest predictive accuracy ($R^2 \geq 0.93$). The prediction of $sDA_{500lx/50\%}$ also reached a high accuracy level (R^2 = 0.87–0.90). UOD, affected by the nonlinearity of spatial form and daylight distribution, proved more difficult to predict, yet still achieved acceptable performance (R^2 = 0.61–0.81). Overall, the MAE remained within ±7% across all indicators, demonstrating that the ANN models can effectively replace conventional simulation engines, reducing single-iteration computation time from approximately 300 min to only a few seconds.

Table 13. Performance evaluation results of the ANN model.

Type	Output Feature	R^2	RMSE	MSE	MAE
Standard Side-Lit Classroom	UOD	0.6162	0.0735	0.0054	0.0563
	$sDA_{500lx/50\%}$	0.9006	0.0963	0.0093	0.0717
	$sGA_{0.35/95\%}$	0.9339	0.0383	0.0015	0.0287
	APMV-mean	0.9996	0.0015	0.0000	0.0012
High Side-Lit Classroom	UOD	0.8079	0.0567	0.0032	0.0444
	$sDA_{500lx/50\%}$	0.8883	0.0916	0.0084	0.0660
	$sGA_{0.35/95\%}$	0.9309	0.0429	0.0018	0.0328
	APMV-mean	0.9977	0.0037	0.0000	0.0029
Skylight-Lit Classroom	UOD	0.7421	0.0661	0.0044	0.0507
	$sDA_{500lx/50\%}$	0.8738	0.0947	0.0090	0.0544
	$sGA_{0.35/95\%}$	0.9521	0.0523	0.0027	0.0394
	APMV-mean	0.9688	0.0209	0.0004	0.0164

Table 14. Predictive value regression analysis.

Type	UOD	$sDA_{500lx/50\%}$	$sGA_{0.35/95\%}$	APMV-Mean
Standard Side-Lit Classroom				
High Side-Lit Classroom				
Skylight-Lit Classroom				

4.3. Assessment and Analysis

The optimization and evaluation process was conducted in two stages, corresponding to the two levels of parametric modeling. In the first stage (Section 4.3.1), based on the parametric model of the overall campus layout established in Section 3.4, the study performed layout optimization for the teaching zone. In the second stage (Section 4.3.2), building upon the classroom cluster parametric model introduced in Section 3.5 and the results from the previous layout optimization, a secondary generation process was carried out to refine the classroom configurations in greater detail.

4.3.1. Stage 1: Layout Optimization

By fitting and analyzing three key indicators—activity accessibility distance $S_r(x)$, average solar irradiance $S_{elei}(x)$, and skylight irradiance $S_{skyi}(x)$—we demonstrate that the optimized classroom layouts significantly enhance students' exposure to natural light during outdoor activities. With increasing simulation iterations, all three indicators showed steady improvements and gradually converged (Figure 12).

For Activity Accessibility Distance $S_r(x)$, compared with the initial schemes, the accessibility distances of all three classroom layouts were substantially reduced. Prior to optimization, the distances generally exceeded 100 m, whereas the optimized averages were reduced to approximately 80 m (standard side-lit), 88 m (high side-lit), and 83 m (skylight-lit). In addition, adjusting the raised height of the playground reduced the travel distance to sports facilities by 10.20–22.89%, which is expected to considerably encourage students' outdoor activity participation during breaks.

For Solar Irradiance $S_{elei}(x)$, $S_{skyi}(x)$, Daylight availability also improved. The average irradiance of standard side-lit, high side-lit, and skylight-lit layouts rose to 130 W/m^2, 122 W/m^2, and 120 W/m^2, with the standard side-lit layout showing the highest relative gain (+13.04%), especially in north-facing daylighting. High side-lit and skylight-lit layouts improved by 6.09% and 5%, respectively. Meanwhile, skylight irradiance increased

modestly, with mean values reaching 257 W/m^2 (high side-lit) and 268 W/m^2 (skylight-lit), providing a foundation for refining massing and reducing central daylight blind zones.

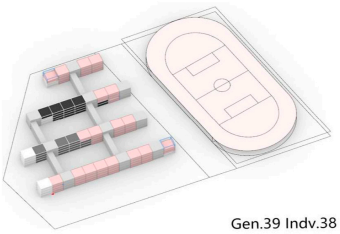
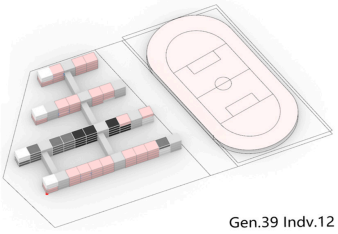
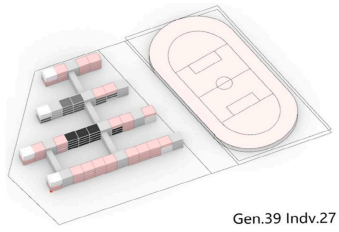
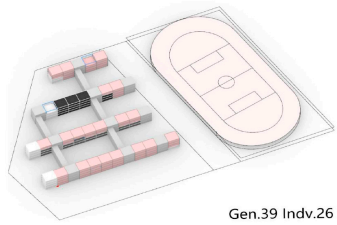
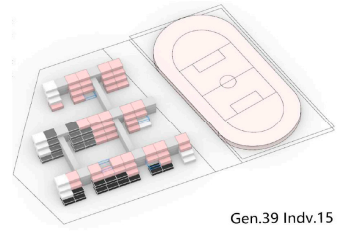
Color Legend		Ordinary Classroom / Corridor Node / Toilet / Office / void volumes / Specialized Classroom / Flexible Classroom							
Type	**Pareto Front Solutions**	**Optimization Results**	**Optimization Objectives**		**Design Variables (Site)**	**Economic & Technical Metrics**			
Standard Side-Lit Classroom	**Overall Optimal Plan A** — Best in Accessible Distance for Activities	 Gen.39 Indv.38	**Accessible Distance for Activities / m**	**76.93**	playground height: 8 m classroom length: 9.6 m classroom width: 8.4 m classroom height: 3.6 m layout_x: 1 layout_y: 2 office_index: 6 special_index: 8 special_layout_z/x: 0 flex_index: 12 flex_layout_z/x: 0 volume_index: 15	**School Scale** /classes	60	**Classroom Area** /m²	8467.2
			Average Solar Irradiance / W/m²	126.14		**Building Height** /m	14.4	**Gross Floor Area** /m²	17529.6
			South-Facing Irradiance / W/m²	166.07		**Floor Area Ratio**	1.03	**Spatial Openness**	0.52
			North-Facing Irradiance / W/m²	86.21		**Building Coverage Ratio**	0.22	**Service Area** /m²	9062.4
	Overall Optimal Plan B — Best in Average Solar Irradiance	 Gen.39 Indv.12	**Accessible Distance for Activities / m**	78.81	playground height: 6 m classroom length: 9.6 m classroom width: 8.4 m classroom height: 3.6 m mlayout_x: 0 layout_y: 2 office_index: 8 special_index: 8 special_layout_z/x: 1 flex_index: 12 flex_layout_z/x: 0 volume_index: 17	**School Scale** /classes	60	**Classroom Area** /m²	8467.2
			Average Solar Irradiance / W/m²	**132.83**		**Building Height** /m	14.4	**Gross Floor Area** /m²	17208.96
			South-Facing Irradiance / W/m²	177.38		**Floor Area Ratio**	1.01	**Spatial Openness**	0.51
			North-Facing Irradiance / W/m²	88.28		**Building Coverage Ratio**	0.21	**Service Area** /m²	8741.76
	Overall Optimal Plan C — Best in Average Performance Across All Indicators	 Gen.39 Indv.27	**Accessible Distance for Activities / m**	**79.72**	playground height: 6 m classroom length: 9.6 m classroom width: 8.4 m classroom height: 3.6 mlayout_x: 0 layout_y: 2 office_index: 8 special_index: 8 special_layout_z/x: 0 flex_index: 8 flex_layout_z/x: 0 volume_index: 17	**School Scale** /classes	60	**Classroom Area** /m²	8467.2
			Average Solar Irradiance / W/m²	**131.79**		**Building Height** /m	14.4	**Gross Floor Area** /m²	17208.96
			South-Facing Irradiance / W/m²	175.91		**Floor Area Ratio**	1.01	**Spatial Openness**	0.51
			North-Facing Irradiance / W/m²	87.67		**Building Coverage Ratio**	0.21	**Service Area** /m²	8741.76
	Overall Optimal Plan D — Best in Average Performance Across All Indicators	 Gen.39 Indv.26	**Accessible Distance for Activities / m**	**80.01**	playground height: 8 m classroom length: 9.6 m classroom width: 8.4 m classroom height: 3.6 mlayout_x: 1 layout_y: 2 office_index: 6 special_index: 5 special_layout_z/x: 1 flex_index: 16 flex_layout_z/x: 0 volume_index: 17	**School Scale** /classes	60	**Classroom Area** /m²	8467.2
			Average Solar Irradiance / W/m²	**129.44**		**Building Height** /m	14.4	**Gross Floor Area** /m²	17529.6
			South-Facing Irradiance / W/m²	171.75		**Floor Area Ratio**	1.03	**Spatial Openness**	0.52
			North-Facing Irradiance / W/m²	84.63		**Building Coverage Ratio**	0.22	**Service Area** /m²	9062.4
High Side-Lit Classroom	**Overall Optimal Plan A** — Best in Accessible Distance for Activities	 Gen.39 Indv.15	**Accessible Distance for Activities / m**	**78.61**	playground height: 6 m classroom length: 9.6 m classroom width: 8.4 m classroom height: 3.9 m layout_x: 0 layout_y: 4 office_index: 9 special_index: 9 special_layout_z/x: 0 flex_index: 18 flex_layout_z/x: 1 volume_index: 1	**School Scale** /classes	48	**Classroom Area** /m²	6773.76
			Average Solar Irradiance / W/m²	120.53		**Building Height** /m	15.6	**Gross Floor Area** /m²	14065.92
			South-Facing Irradiance / W/m²	175.26		**Outdoor Activity Area** /m²	2540.16	**Spatial Openness**	0.52
			North-Facing Irradiance / W/m²	65.8		**Floor Area Ratio**	0.83	**Service Area** /m²	7292.16
			Roof Solar Irradiance / W/m²	258.05		**Building Coverage Ratio**	0.39	/	/

Figure 12. *Cont.*

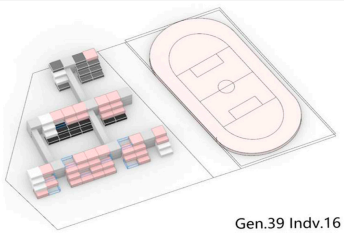
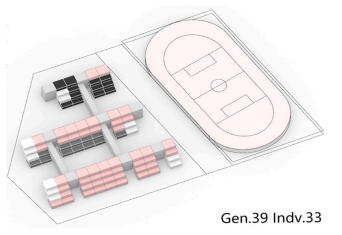
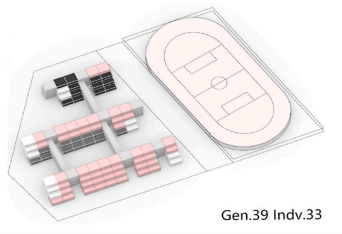
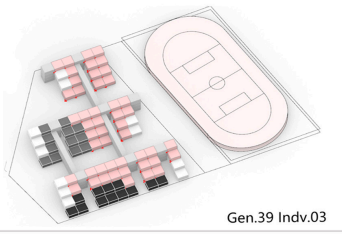
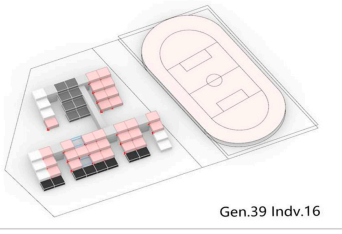
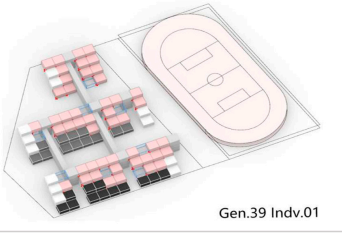
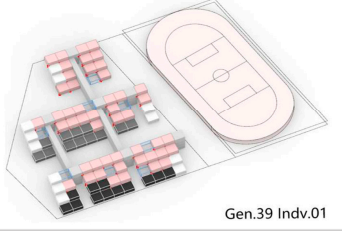
Color Legend	Ordinary Classroom / Corridor Node / Toilet / Office / void volumes / Specialized Classroom / Flexible Classroom				Design Variables (Site)	Economic & Technical Metrics			
Type	**Pareto Front Solutions**	**Optimization Results**	**Optimization Objectives**						
High Side-Lit Classroom	**Overall Optimal Plan B** — Best in Average Solar Irradiance	 Gen.39 Indv.16	Accessible Distance for Activities / m	93.96	playground height: 6 m classroom length：9.6 m classroom width：8.4 m classroom height：3.9 m mlayout_x: 0 layout_y: 1 office_index: 9 special_index: 8 special_layout_z/x: 1 flex_index: 16 flex_layout_z/x: 1 volume_index: 1	**School Scale** /classes	36	**Classroom Area** /m²	5080.32
			Average Solar Irradiance / W/m²	**127.44**		**Building Height** /m	15.6	**Gross Floor Area** /m²	11203.2
			South-Facing Irradiance / W/m²	180.89		**Outdoor Activity Area** /m²	1905.12	**Spatial Openness**	0.55
			North-Facing Irradiance / W/m²	73.99		**Floor Area Ratio**	0.66	**Service Area** /m²	6122.8
			Roof Solar Irradiance / W/m²	259.76		**Building Coverage Ratio**	0.34	/	/
	Overall Optimal Plan C — Best in Roof Solar Irradiance	 Gen.39 Indv.33	Accessible Distance for Activities / m	94.8	playground height: 6 m classroom length：9.6 m classroom width：8.4 m classroom height：3.9 m mlayout_x: 1 layout_y: 3 office_index: 8 special_index: 8 special_layout_z/x: 1 flex_index: 16 flex_layout_z/x: 1 volume_index: 1	**School Scale** /classes	48	**Classroom Area** /m²	6773.76
			Average Solar Irradiance / W/m²	122.41		**Building Height** /m	15.6	**Gross Floor Area** /m²	14065.92
			South-Facing Irradiance / W/m²	171.94		**Outdoor Activity Area** /m²	2540.16	**Spatial Openness**	0.52
			North-Facing Irradiance / W/m²	72.88		**Floor Area Ratio**	0.83	**Service Area** /m²	7292.16
			Roof Solar Irradiance / W/m²	**264.42**		**Building Coverage Ratio**	0.41	/	/
High Side-Lit Classroom	**Overall Optimal Plan D** — Best in Average Performance Across All Indicators	 Gen.39 Indv.33	**Accessible Distance for Activities / m**	**90.85**	playground height: 6 m classroom length：9.6 m classroom width：8.4 m classroom height：3.9 m mlayout_x: 1 layout_y: 4 office_index: 9 special_index: 16 special_layout_z/x: 1 flex_index: 18 flex_layout_z/x: 1 volume_index: 1	**School Scale** /classes	48	**Classroom Area** /m²	6773.76
			Average Solar Irradiance / W/m²	**127.41**		**Building Height** /m	15.6	**Gross Floor Area** /m²	14065.92
			South-Facing Irradiance / W/m²	180.86		**Outdoor Activity Area** /m²	2540.16	**Spatial Openness**	0.52
			North-Facing Irradiance / W/m²	73.95		**Floor Area Ratio**	0.83	**Service Area** /m²	7292.16
			Roof Solar Irradiance / W/m²	**262.55**		**Building Coverage Ratio**	0.38	/	/
Skylight-Lit Classroom	**Overall Optimal Plan A** — Best in Accessible Distance for Activities	 Gen.39 Indv.03	**Accessible Distance for Activities / m**	**79.83**	playground height: 6 m classroom length：9.0 m classroom width：7.8 m classroom height：3.9 m layout_x: 0 layout_y: 4 office_index: 9 special_index: 9 special_layout_z/x: 0 flex_index: 11 flex_layout_z/x: 1 volume_index: 2	**School Scale** /classes	48	**Classroom Area** /m²	6773.76
			Average Solar Irradiance / W/m²	117.1		**Building Height** /m	15.6	**Gross Floor Area** /m²	14065.92
			South-Facing Irradiance / W/m²	172.4		**Outdoor Activity Area** /m²	2540.16	**Spatial Openness**	0.52
			North-Facing Irradiance / W/m²	61.8		**Floor Area Ratio**	0.83	**Service Area** /m²	7292.16
			Roof Solar Irradiance / W/m²	268.18		**Building Coverage Ratio**	0.38	/	/
	Overall Optimal Plan B — Best in Average Solar Irradiance	 Gen.39 Indv.16	Accessible Distance for Activities / m	85.99	playground height: 6 m classroom length：9.6 m classroom width：8.4 m classroom height：3.9 m layout_x: 1 layout_y: 3 office_index: 8 special_index: 18 special_layout_z/x: 1 flex_index: 12 flex_layout_z/x: 1 volume_index: 2	**School Scale** /classes	30	**Classroom Area** /m²	4354.56
			Average Solar Irradiance / W/m²	**127.65**		**Building Height** /m	15.6	**Gross Floor Area** /m²	8707.2
			South-Facing Irradiance / W/m²	180.77		**Outdoor Activity Area** /m²	3265.92	**Spatial Openness**	0.5
			North-Facing Irradiance / W/m²	74.54		**Floor Area Ratio**	0.51	**Service Area** /m²	4352.64
			Roof Solar Irradiance / W/m²	272.85		**Building Coverage Ratio**	0.38	/	/
	Overall Optimal Plan C — Best in Roof Solar Irradiance	 Gen.39 Indv.01	Accessible Distance for Activities / m	84.74	playground height: 6 m classroom length：9.0 m classroom width：7.8 m classroom height：3.9 m layout_x: 0 layout_y: 4 office_index: 3 special_index: 9 special_layout_z/x: 1 flex_index: 13 flex_layout_z/x: 1 volume_index: 5	**School Scale** /classes	48	**Classroom Area** /m²	5896.8
			Average Solar Irradiance / W/m²	127.4		**Building Height** /m	15.6	**Gross Floor Area** /m²	12328.2
			South-Facing Irradiance / W/m²	181.24		**Outdoor Activity Area** /m²	4422.6	**Spatial Openness**	0.52
			North-Facing Irradiance / W/m²	73.56		**Floor Area Ratio**	0.73	**Service Area** /m²	6431.4
			Roof Solar Irradiance / W/m²	**273.32**		**Building Coverage Ratio**	0.52	/	/
	Overall Optimal Plan D — Best in Average Performance Across All Indicators	 Gen.39 Indv.01	**Accessible Distance for Activities / m**	**81.37**	playground height: 6 m classroom length：9.0 m classroom width：7.8 m classroom height：3.9 m mlayout_x: 1 layout_y: 4 office_index: 9 special_index: 5 special_layout_z/x: 1 flex_index: 13 flex_layout_z/x: 1 volume_index: 2	**School Scale** /classes	48	**Classroom Area** /m²	5896.8
			Average Solar Irradiance / W/m²	**126.01**		**Building Height** /m	15.6	**Gross Floor Area** /m²	12609
			South-Facing Irradiance / W/m²	180.77		**Outdoor Activity Area** /m²	4422.6	**Spatial Openness**	0.53
			North-Facing Irradiance / W/m²	74.54		**Floor Area Ratio**	0.74	**Service Area** /m²	6712.2
			Roof Solar Irradiance / W/m²	**272.16**		**Building Coverage Ratio**	0.52	/	/

Figure 12. Layout optimization results of three classroom clusters layout.

Each optimized scheme comprehensively reported Economic and Technical Indicators, including FAR, building density, spatial openness, and gross floor area, providing a systematic reference framework for manual evaluation and scheme selection within the Pareto front. Due to differences in setback distances associated with the three classroom types, the floor area ratio was highest in standard side-lit layouts, followed by high side-lit and skylight-lit layouts; in contrast, building density was greatest for skylight-lit layouts, followed by high side-lit, and lowest for standard side-lit. Regarding school scale, the standard side-lit classroom layouts could accommodate up to 60 classes, demonstrating higher spatial efficiency, whereas the high side-lit and skylight-lit layouts accommodated 30–48 classes. Notably, the setback design of the high side-lit and skylight-lit layouts created more than 2000 m^2 of proximate outdoor activity space, which helps extend students' exposure to sunlight and promotes healthier growth.

4.3.2. Stage 2: Classroom Clusters Optimization

Building upon the first stage of layout optimization, this experiment further focuses on detailed structural optimization for standard classrooms characterized by long average usage duration, high daylighting requirements, and intensive occupancy rates. In this process, a unified construction and internal morphology replaced the simplified hexahedral model used previously, ensuring the feasibility of the schemes in real scenarios. At this stage, the D-schemes of three layouts were selected as the optimization basis, and the mean values of four performance indicators across dozens of classrooms in each cluster were iteratively optimized.

For Standard Side-Lit Classroom (Figure 13a), UOD stabilized at 0.46, with some solutions surpassing the 0.50 threshold. sDA increased markedly from 0.23 to 0.53 (+130%), greatly enhancing daylight utilization, while sGA declined slightly from 0.83 to 0.75, striking a balance between improved daylight and glare control. APMV remained around 0.44, indicating limited thermal impact. For High Side-Lit Classroom (Figure 13b), UOD rose from 0.36 to 0.50 (+39%), with some solutions reaching 0.66. sGA improved from 0.53 to 0.69 (+30%), reducing glare substantially, while sDA increased modestly to 0.55, with certain solutions exceeding 0.70. Meanwhile, APMV fell from 0.51 to 0.47 (–7.8%), mitigating overheating from south-facing windows. For Skylight-Lit Classroom (Figure 13c), UOD improved from 0.40 to 0.50 (+20%), while sGA surged from 0.47 to 0.80 (+70%), nearly eliminating glare issues. Although sDA declined from 0.82 to 0.65 due to trade-offs with UOD and sGA, it remained above the 0.50 benchmark, with some solutions close to 0.80. APMV decreased from 0.59 to 0.51 (–13.6%), with a few cases below 0.40, alleviating skylight overheating.

Based on the optimization results, the experiment applied the K-means clustering algorithm to classify the solution sets. According to the optimization tendencies of classroom design parameters, each type of classroom was divided into 4 categories, and one representative solution was selected from each category to further explore the refined design strategies proposed by the algorithm and evaluate their effects on daylighting and thermal performance.

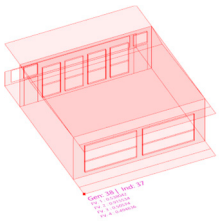
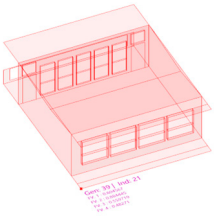
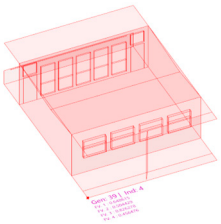
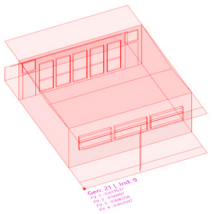
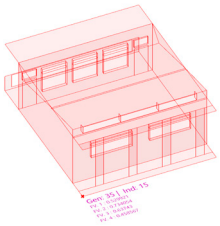
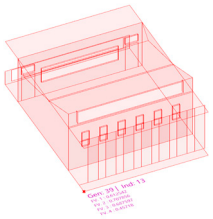
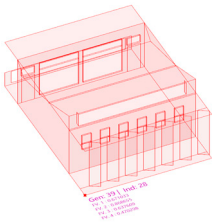
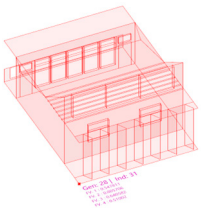
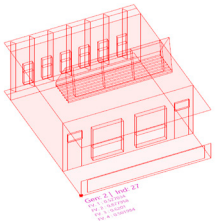
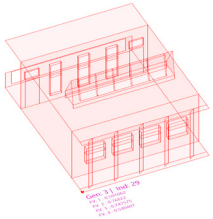
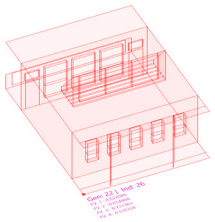
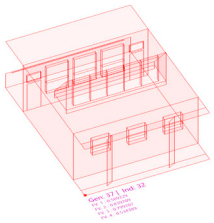


Figure 13. Optimization process of classroom cluster indicators: (**a**) Standard side-lit classroom, (**b**) High side-lit classroom, (**c**) Skylight-lit classroom.

The generated schemes exhibited certain common features: in Standard Side-Lit Classrooms, the south-facing façades generally lacked vertical louvers, and were equipped only with narrow horizontal shading devices; corridors were located on the north side, with semi-outdoor solid walls or glass balustrades. In High Side-Lit Classrooms, the south façades had dense vertical louvers, the north-side corridors adopted semi-outdoor glass balustrades, and the north wall had significantly more window area than the south wall. In

Skylight-Lit Classrooms, skylights were relatively high, but shading treatments for side windows and skylight apertures varied considerably (Table 15).

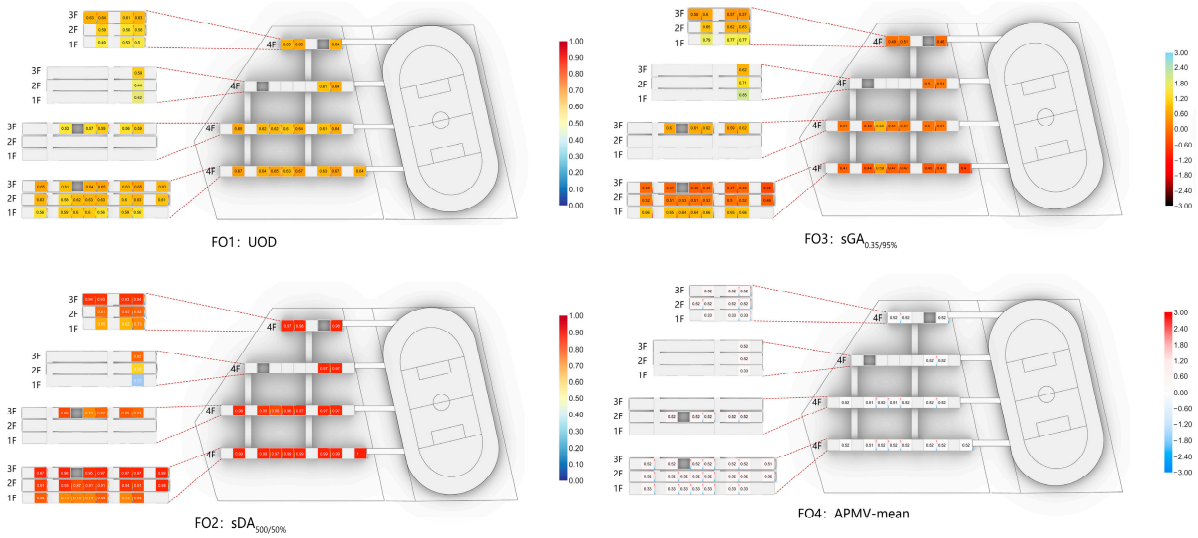
Table 15. Pareto front solutions for clusters optimization of classroom parameters **(The indicator is the average of all classrooms in the cluster)**.

Type	A	B	C	D
	UOD/sDA/sGA/APMV			
Standard Side-Lit Classroom				
Value	0.54/**0.92**/0.51/0.49	**0.65**/0.50/**0.83**/0.46	0.60/**0.88**/0.56/0.48	**0.64**/0.51/**0.81**/0.45
High Side-Lit Classroom				
Value	0.53/**0.73**/0.64/0.46	0.61/**0.71**/**0.69**/0.46	**0.67**/**0.87**/0.64/0.47	0.55/**0.81**/0.64/0.51
Skylight-Lit Classroom				
Value	0.53/**0.88**/0.62/0.50	0.50/0.77/0.75/0.54	**0.63**/**0.85**/0.77/0.54	0.57/**0.84**/**0.80**/0.53

Across the selected stage 2 optimization results—Standard Side-Lit Classroom B Cluster (Figure 14), High-Lit Classroom C Cluster (Figure 15) and Skylight-Lit Classroom C Cluster (Figure 16)—distinct spatial patterns of daylighting and thermal performance emerge depending on their layout positions within the cluster.

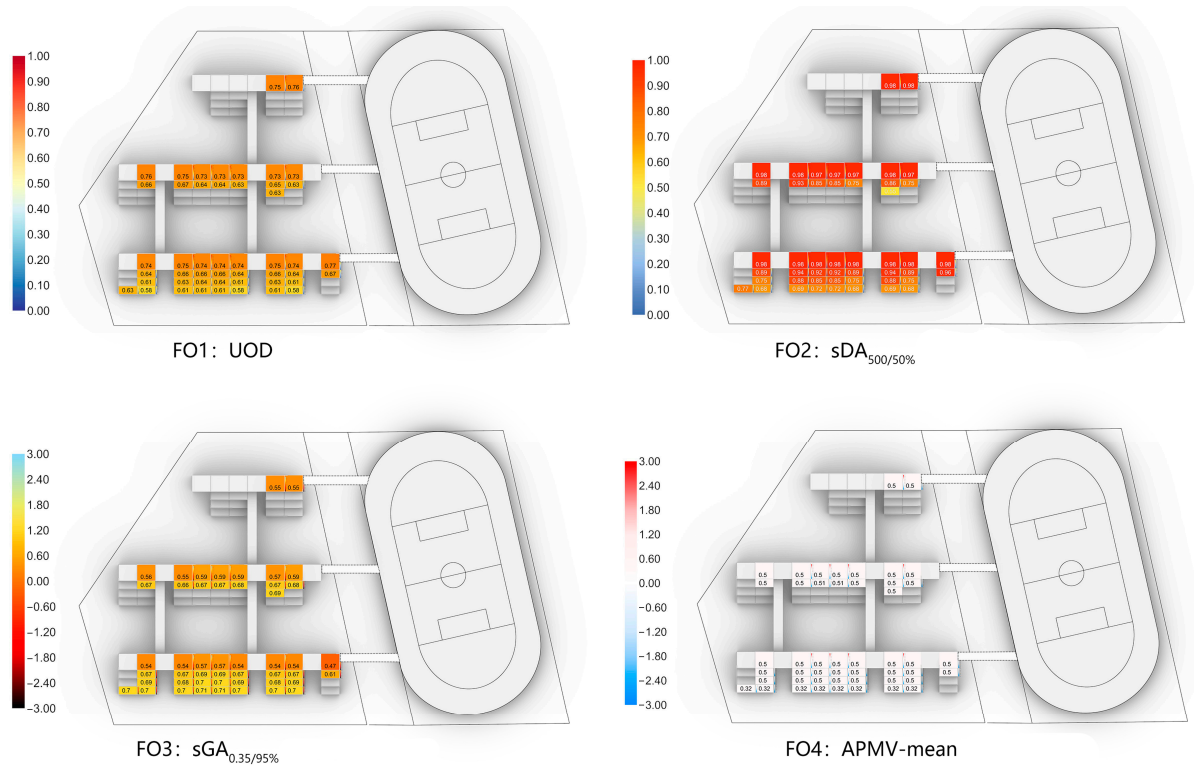
In the standard side-lit classrooms, daylight quality is strongly influenced by mutual shading and building orientation. Lower floors and rear rows tend to experience insufficient daylight, while the façades facing east or west are more prone to glare and uneven brightness. This layout demonstrates a clear depth-related gradient in both daylight distribution and visual comfort, revealing the limitations of lateral illumination in deep-plan clusters.

The high side-lit classrooms perform more consistently across different floors and rows. The elevated window configuration allows daylight to penetrate deeper into the space, reducing the dependence on building orientation and minimizing shadowing effects from adjacent units. As a result, overall illuminance uniformity and glare control remain relatively stable throughout the cluster, even in mid- or lower-level classrooms.



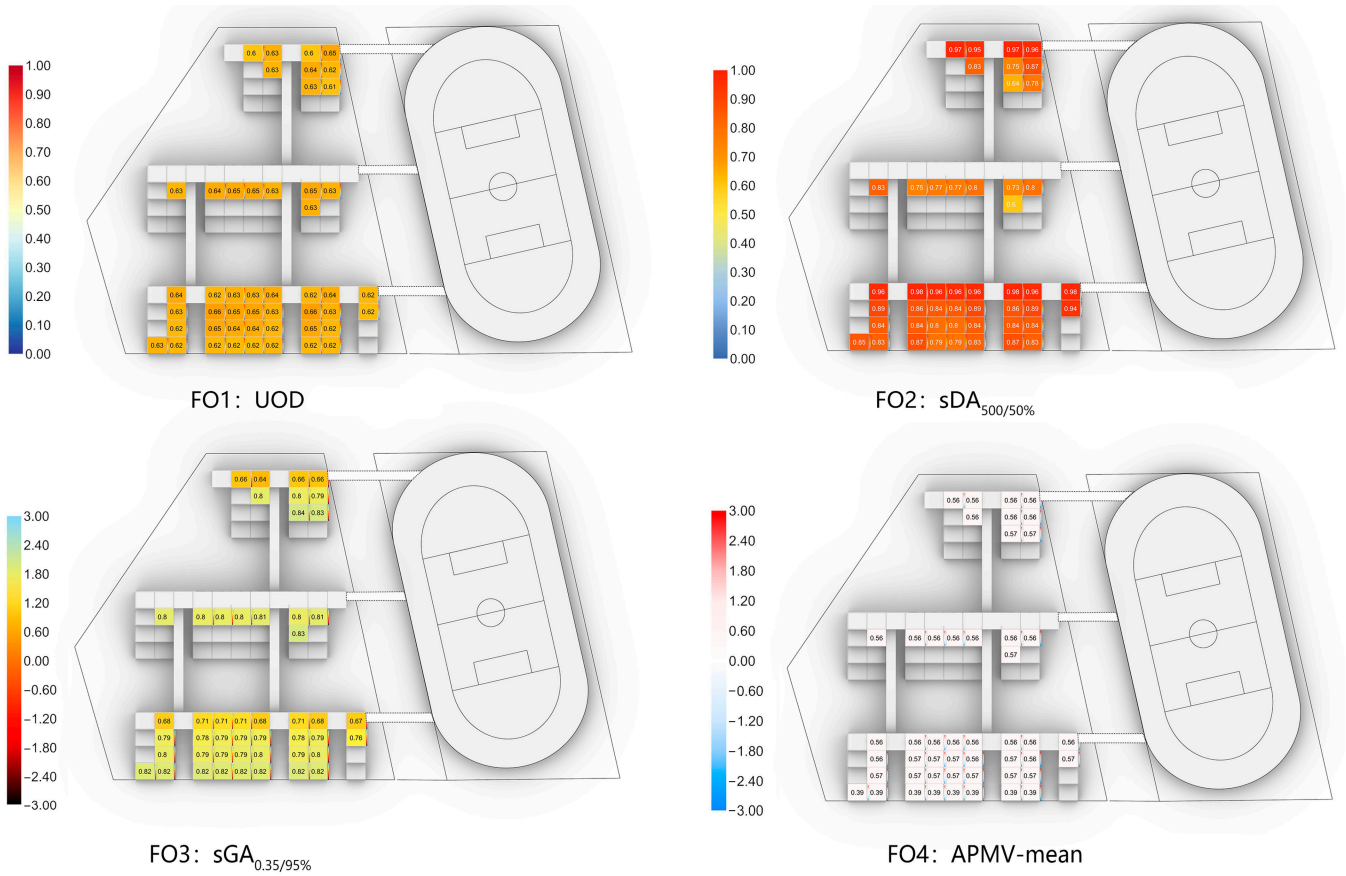
Optimization Results		Classroom Design Parameter									
UOD	sDA500	SH	CGC	CGT	NWC	NHWWR	NVWWR	NWSH	SWC	SHWWR	SVWWR
0.6	**0.88**	1.2	2	0.1	2	0.9	0.9	0.6	6	0.5	0.4
sGA	**APMV**	**SWSH**	**COW**	**COT**	**COWR**	**SW**	**VBC**	**VBW**	**VBRA**	**CTLPF**	**CTH**
0.56	**0.48**	1	2.1	0	1	1.8	7	0.8	60	0.8	0.9

Figure 14. Standard Side-Lit Classroom B Cluster—Overview of 60 Classrooms' Indicators, Parameters, and Optimization Results.



Optimization Results		Classroom Design Parameter									
UOD	sDA500	NWC	NHWWR	NVWWR	NWSH	SWC	SHWWR	SVWWR	SWSH	COW	COT
0.67	**0.87**	2	0.9	0.9	0.6	6	0.5	0.4	1	2.1	0
sGA	**APMV**	**COWR**	**SW**	**VBC**	**VBW**	**VBRA**	**CTLPF**	**CTH**	**SH**	**CGC**	**CGT**
0.64	**0.47**	1	1.8	7	0.8	60	0.8	0.9	1.2	2	0.1

Figure 15. High-Lit Classroom C Cluster—Overview of 48 Classrooms' Indicators, Parameters, and Optimization Results.



Optimization Results		Classroom Design Parameter											
UOD	**sDA500**	**NWC**	**NHWWR**	**NVWWR**	**NWSH**	**SWC**	**SHWWR**	**SVWWR**	**SWSH**	**COW**	**COT**	**COO**	**COWR**
0.63	**0.85**	3	0.8	0.8	0.7	3	0.5	0.5	0.8	2.4	0	1	2
sGA	**APMV**	**SW**	**VBC**	**VBW**	**VBRA**	**SH**	**SS**	**NS**	**ES**	**WS**	**SA**	**CGC**	**CGT**
0.77	**0.54**	1.2	2	0.6	−30	2.4	2.4	3.6	1.2	1.2	0	6	0.1

Figure 16. Skylight-Lit Classroom C Cluster—Overview of 48 Classrooms' Indicators, Parameters, and Optimization Results.

By contrast, the skylight-lit classrooms exhibit the most homogeneous performance across all spatial positions. Since the primary light source is vertical, the influence of external obstruction and façade orientation becomes minimal. Daylight distribution remains even across floors and rows, and visual comfort is well maintained. However, top-floor classrooms may experience slightly elevated thermal loads due to direct solar exposure, requiring refined shading or ventilation measures.

Overall, the comparison indicates that while side-lit configurations are highly sensitive to spatial position and surrounding obstructions, high side-lit and skylight systems significantly reduce this dependency, achieving greater daylight uniformity and comfort at the cluster scale.

4.4. Performance Comparison

This section provides a comprehensive analysis of average daylighting performance, uniformity, glare control, and thermal comfort across three classroom clusters. The aim is to reveal the differences in performance under multi-objective optimization and to explain their underlying causes (Figure 17).

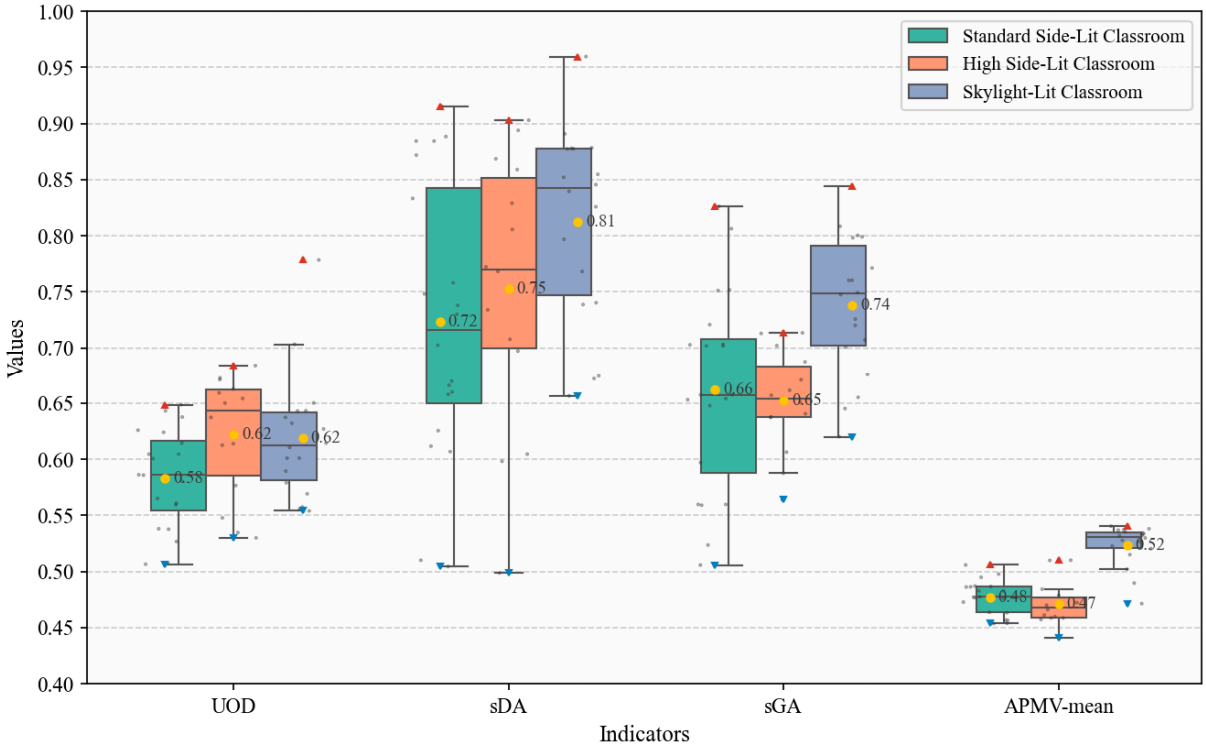


Figure 17. Performance comparison of layout optimization for three classroom types.

Across all indicators, the skylight-lit classroom demonstrated the most balanced and superior daylight performance, while the high side-lit classroom achieved stable results with improved uniformity and glare control, and the standard side-lit classroom showed acceptable yet position-sensitive outcomes. In terms of daylight uniformity (UOD), both skylight-lit and high side-lit schemes effectively reduced brightness gradients through deeper light penetration and ceiling reflection, outperforming the side-lit model constrained by unilateral illumination. For spatial daylight autonomy (sDA), skylight-lit classrooms provided the widest light coverage and maintained adequate illuminance even in deeper zones, while high side-lit spaces offered moderate improvement and side-lit ones showed the steepest light decay. Regarding glare control (sGA), skylights—with optimized louvers and diffused top lighting—achieved the best balance between brightness and visual comfort, followed by high side-lit designs; side-lit layouts remained more prone to low-angle glare, especially on west-facing façades. In thermal performance (APMV), however, skylight-lit classrooms exhibited slightly higher heat gain, whereas side-lit and high side-lit designs benefited from better ventilation and lower thermal discomfort. Overall, the results highlight that while skylight systems maximize daylight quality and visual comfort, side- and high side-lit configurations retain thermal advantages, suggesting the need for hybrid strategies in future classroom design.

Skylight-lit classrooms demonstrated clear advantages in daylight sufficiency and glare control, making them suitable for teaching spaces that prioritize balanced daylight distribution and visual comfort. High side-lit classrooms offered a better compromise between daylight uniformity and thermal comfort, particularly effective in deeper classroom layouts. Standard side-lit classrooms, though less competitive in daylighting performance, provided unique advantages in natural ventilation and thermal regulation, which is particularly valuable in hot-humid climates where reliance on mechanical cooling should be minimized. These comparative findings provide targeted parametric optimization strategies for classroom design under varying climatic conditions and spatial scales.

5. Discussion

5.1. An Optimization Framework Bridging Macro and Micro Scales

The core contribution of this study lies in establishing a dual-layer design framework that bridges campus-scale functional layout (macro) and classroom-scale architectural configuration (micro). In architectural research, designing across scales has long been a fundamental challenge—how to integrate urban block-level planning decisions with building-level components within a unified parametric logic [72]. Unlike most existing studies that optimize building performance at a single scale, prior works tend to either focus on envelope-level parameters—such as window-to-wall ratio, geometry, or orientation—to enhance daylighting and energy efficiency [73], or address urban morphology optimization to balance solar access, energy use, and spatial quality [74]. However, these approaches often neglect the micro-environmental conditions within individual buildings. A structure poorly oriented or shaded in the early layout stage inevitably limits its daylighting potential, regardless of how refined its façade design may later become. Conversely, the macro-level optimization framework developed in this study enhances the solar potential of each building envelope, thereby increasing the likelihood of achieving superior performance in subsequent design stages. This computational workflow effectively overcomes the conventional separation between scales and decisions, offering a systematic approach to achieving global performance optimization in campus design.

Beyond its methodological advantages, this framework represents a paradigm shift—from a traditional, linear, and fragmented design process toward an integrated, performance-driven one [75]. In conventional practice, master planning and building design are often treated as discrete stages: planners determine site boundaries and basic volumes, while architects work within those constraints. Such separation frequently leads to suboptimal outcomes, as macro-level decisions fail to quantitatively anticipate their downstream impacts on micro-level environmental performance. The proposed framework establishes a causal linkage between design phases, where the first-stage optimization objectives (solar radiation and accessibility) directly inform and enable the second-stage goals (daylighting and thermal comfort). This creates a concurrent design thinking mechanism that computationally bridges disciplinary boundaries, intertwining macro and micro considerations into a unified optimization process [76]. As a result, the approach delivering a data-informed solution aligned with the broader call for integrating form, function, environment, and culture in complex planning tasks [77].

5.2. A Goal-Driven Paradigm for Daylighting School Design

This study incorporated activity accessibility distance as a key objective function in the stage 1 optimization. While its primary purpose was to increase students' exposure to outdoor sunlight and enhance the overall efficiency of natural light utilization, this parameter extends beyond conventional optimization goals centered solely on physical environmental performance [78]. It introduces user behavior and spatial experience as integral design considerations [79,80]. In campus planning, spatial quality is defined not only by environmental comfort but also by the extent to which it supports teaching, social interaction, and daily activities [81]. Issues such as traffic congestion, segregated functional zones, and inactive public spaces remain prevalent in contemporary campus design [82]. By quantifying accessibility as an optimization objective, this study directly addresses real-world problems—such as the limited use of sports facilities due to excessive travel distances—highlighted in the introduction.

This approach aligns with the long-standing use of accessibility as a key metric in industrial layout optimization and urban space syntax analysis [83]. More importantly, it advocates a goal-driven rather than form-driven design philosophy. Traditional campus

design often begins with formal precedents or stylistic preferences, whereas this research starts from a fundamental redefinition of what constitutes a "Daylighting School": one that ensures ample daylight potential, convenient outdoor pathways, and healthy, comfortable classrooms. These qualitative expectations are rigorously encoded into quantifiable, computational objectives, enabling algorithms to identify spatial configurations and geometries that best fulfill these design intentions [84,85].

5.3. Advanced Daylighting Strategies

The second-stage results of this study provide empirical evidence for the superior performance of daylighting strategies in classrooms. As shown in Table 16, compared with the standard side-lit model widely used in Chinese schools, both the high side-lit and skylight-lit configurations demonstrate remarkable advantages in enhancing illuminance uniformity and mitigating glare—issues that are particularly critical in deep classrooms of high-density urban campuses.

Table 16. Comparative Analysis of Classroom Daylighting Strategy Performance.

Strategy Type	Spatial Daylight Autonomy (sDA)	Glare Acceptability (sGA)	Illuminance Uniformity	Key Advantage	Key Challenge
Standard Side-Lit	Low in areas distant from the window	Low near the window; high glare risk	Low, with significant gradient	Cost-effective, simple construction, provides external view	Uneven light distribution; insufficient daylight in deep zones
High Side-Lit	Generally higher, with significant improvement in deep areas	High; effectively controls low-angle glare	High; markedly improves uniformity	Introduces diffuse skylight; enhances illuminance in deep spaces	Requires complex structural design; may affect façade aesthetics
Skylight-Lit	Highest overall; independent of building orientation	Highest; low glare risk after optimization	Highest; most uniform light distribution	Provides sufficient daylight for deep-plan or core spaces	High initial cost and waterproofing requirements; risk of overheating

By introducing daylight from higher positions, the high side-lit and skylight-lit systems allow light to penetrate deeper into the room, achieving more uniform distribution (higher UOD) and significantly improving the overall daylighting quality [86]. In terms of glare control, although poorly designed skylights can become potential sources of glare, the optimized skylight-lit configuration in this study demonstrated superior performance in spatial glare acceptability (sGA). This improvement primarily stems from the higher incident angle of top lighting, which reduces low-angle, high-luminance direct light entering the visual field—one of the main causes of visual discomfort [87]. Heschong Mahone [88] studies deliberately isolated the effect of daylight illumination from other visual variables such as exterior views and found a strong positive correlation between pure daylight exposure and students' academic performance. From a building performance perspective, the present study provides a scientific explanation for this phenomenon: a well-designed top-lighting system can deliver abundant and uniformly distributed daylight while effectively mitigating glare risks, thereby creating an indoor luminous environment that genuinely supports visual comfort, cognitive focus, and learning efficiency.

5.4. Limitations and Future Work

This study has made progress in exploring generative design approaches for campus planning; however, several limitations remain. First, the flexibility of the generative design process is limited. The current "Daylighting School" generation framework is still in its early experimental stage. The design rules are relatively rigid, leading to solutions that tend to be mechanical and lack diversity and spatial fluidity. Second, thermal comfort

indicators are not sufficiently considered. The study primarily focused on daylighting performance, while the assessment of thermal conditions was relatively simplified and did not fully capture the complexity of real indoor thermal environments. Third, the functional coverage of the generative process remains restricted. The present research focuses mainly on the teaching zone, excluding other essential campus facilities such as canteens and administrative buildings. As a result, the framework requires manual functional zoning by architects, which constrains its applicability to broader design scenarios.

Building on these limitations, future work can be advanced in several directions. First, the research scope should be extended to campuses located in diverse climatic and cultural contexts to establish a more universal "Daylighting School" design model and parameter system. Further investigation is also needed to explore how coupled light–thermal environments affect students' learning efficiency and psychological well-being. In addition, incorporating metrics such as indoor acoustic comfort, life-cycle cost (LCC), and carbon emissions (LCC/LCA) would enable the development of a more holistic, sustainability-oriented optimization platform. Second, advanced computational methods such as deep reinforcement learning (e.g., XGB/GP) and agent-based modeling could be integrated to enhance the predictive accuracy and generalization of the models. Virtual reality (VR) technologies could also be utilized to create immersive design assessment environments, providing designers with intuitive, real-time feedback. Finally, collaboration with educational authorities and design institutions would allow the "Daylighting School" design concept and the proposed generative platform to be applied in real-world projects. Field implementation and data accumulation could, in turn, help validate, refine, and expand the research outcomes, promoting the broader adoption of daylight-oriented campus design practices through academic dissemination and case-based demonstration.

6. Conclusions

This study proposes a daylight-oriented design model for primary and secondary school campuses under the "Daylighting School" concept, aiming to balance indoor daylighting and outdoor activity opportunities. A two-stage generative optimization framework was developed, integrating Artificial Neural Networks (ANNs) and NSGA-II with daylight autonomy, glare, uniformity, and thermal comfort incorporated into a unified multi-objective system. The framework not only reveals performance differences and underlying mechanisms among alternative daylighting strategies but also demonstrates the effectiveness of generative algorithms in supporting complex architectural decision-making, providing a replicable methodology for performance-driven school design.

At the experimental level, the research began with an analysis of current daylighting conditions in Chinese classrooms, referencing the "Daylighting School" guidelines and international precedents to propose a strategy of "adjacent outdoor spaces + combined skylight and side-lighting". A two-stage optimization was then conducted on a typical school site in Guangzhou. Stage 1 focused on overall building layout, optimizing solar radiation and accessibility distances; results showed a 5–20% improvement in both daylight access and outdoor circulation efficiency compared to baseline schemes. Stage 2 refined classroom clusters, with ANN accelerating the evaluation of sDA, sGA, UOD, and APMV-mean. Results confirmed that High Side-Lit and Skylight-Lit classrooms outperformed Standard Side-Lit classrooms in terms of illuminance, uniformity, and glare control while maintaining acceptable thermal comfort levels, thus validating the feasibility and advantages of the "Daylighting School" model in the Lingnan climate.

At the practical level, this research provides a parametric design framework and operable optimization pathway for the implementation of "Daylighting Schools" in Lingnan, enabling architects to balance daylighting and thermal conditions across varying spatial

scales and climatic contexts. Beyond the regional scope, the framework demonstrates cross-regional and cross-typological applicability, offering a valuable reference for educational facilities in high-density urban environments and extending the application boundary of artificial intelligence in architectural design.

Author Contributions: H.S.: software, validation, investigation, data curation, writing—original draft preparation, visualization, writing—original draft preparation. Y.L.: conceptualization, methodology, validation, resources, supervision, project administration, writing—review and editing, funding acquisition. Q.D.: validation, formal analysis, resources, writing—original draft preparation. All authors have read and agreed to the published version of the manuscript.

Funding: This research received no external funding.

Institutional Review Board Statement: Ethics approval was waived because the survey was administered anonymously via the Wenjuanxing platform (https://www.wjx.cn/, accessed on 8 January 2024), in compliance with regulatory requirements; the questionnaire link was non-traceable and collected no direct or indirect identifiers. No names, gender, contact details, IDs, IP addresses, health/medical/psychological data, political opinions, religious beliefs, or any other sensitive personal information were collected; responses were analyzed only in aggregate.

Informed Consent Statement: Informed consent for participation was obtained from all subjects involved in the study.

Data Availability Statement: The original contributions presented in this study are included in the article. Further inquiries can be directed to the corresponding author.

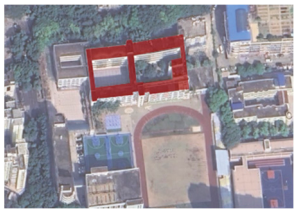
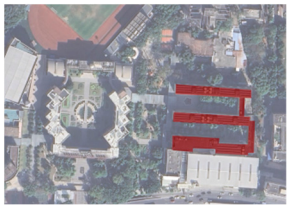
Conflicts of Interest: The authors declare no conflicts of interest.

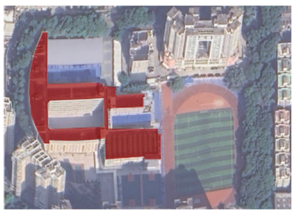
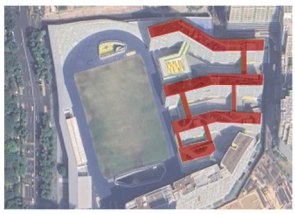
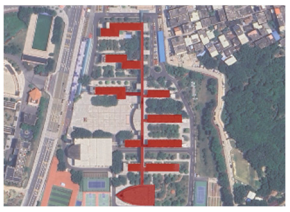
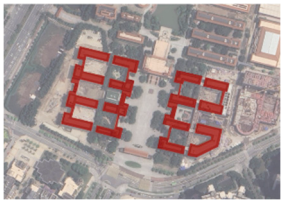
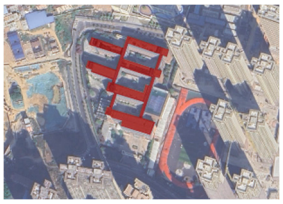
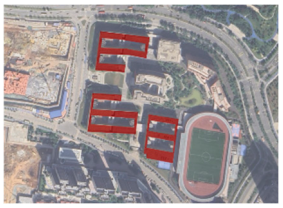
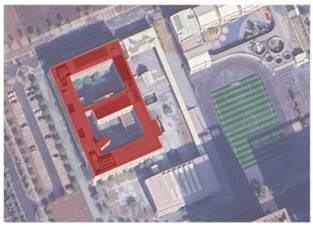
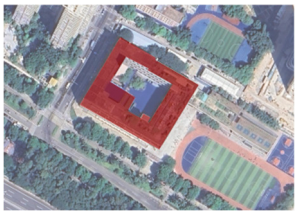
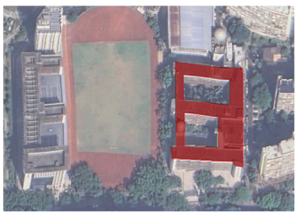
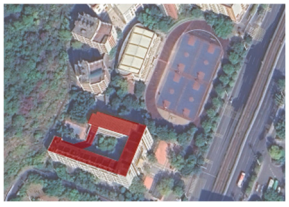
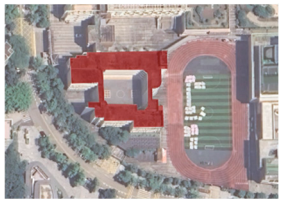
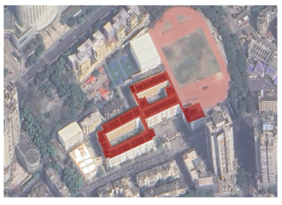
Abbreviations

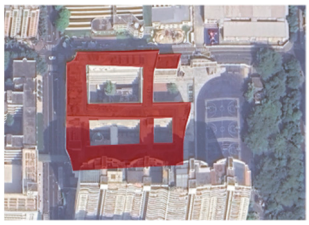
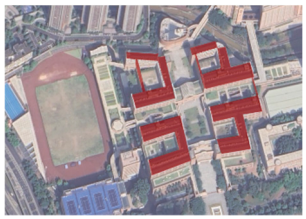
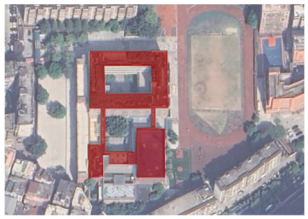
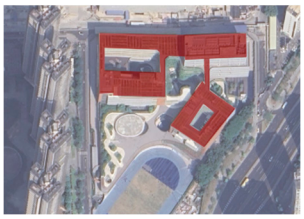
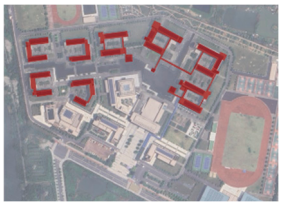
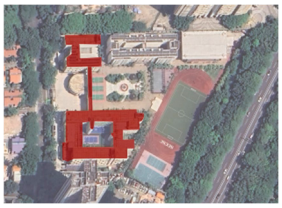
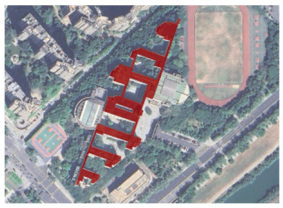
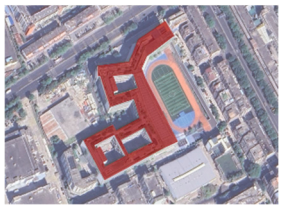
The following abbreviations are used in this manuscript:

E	Illuminance, lx
DF	Daylight Factor, %
DA	Daylight Autonomy, %
UOD	Uniformity of Daylight, %
sDA	Spatial Daylight Autonomy, %
DGP	Disability Glare Probability, %
sGA	Spatial Glare Autonomy, %
APMV	Adaptive Predicted Mean Vote

Appendix A. Design Cases of Teaching Buildings in Guangzhou–Shenzhen Region

Linear Matrix layout Teaching Building Cases			
			
Hongling Experimental School, Shenzhen, CLS = 38, FAR = 0.91	The Affiliated High School of SCNU, CLS = 36, FAR = 0.29	Xinsha School, Shenzhen, CLS = 40, FAR = 3.26	Hongling Middle School, Shenzhen, CLS = 34, FAR = 1.97

Linear Matrix layout Teaching Building Cases			
			
Yunding School, Shenzhen, CLS = 42, FAR = 0.82	Shenzhen Oasis International School, CLS = 36, FAR = 0.73	Futian Middle School, Shenzhen, CLS = 60, FAR = 2.93	Jinlong School, Nansha District, Guangzhou, CLS = 130, FAR = 0.39
			
Guangzhou Foreign Language School, CLS = 60, FAR = 0.88	Guangzhou Nansha No. 1 High School, CLS = 52, FAR = 0.59	The Affiliated Huangpu Experimental School, SCNU, CLS = 29, FAR = 1.03	Guangzhou Experimental Middle School, CLS = 90, FAR = 1.50
Courtyard Layout Teaching Building Cases			
			
The Affiliated Primary School of SCUT (Guangzhou International Campus), CLS = 24, FAR = 0.060	Hongling Experimental School (Shangsha Campus), Shenzhen, CLS = 40, FAR = 0.79	Shenzhen Experimental School (Middle School Section), CLS = 42, FAR = 2.00	Shenzhen Primary School, CLS = 36, FAR = 2.37
			
Suyuan School (West Campus), Huangpu District, Guangzhou, CLS = 18, FAR = 2.30	Nanshan Foreign Language School (Group) Keyuan School, Shenzhen, CLS = 54, FAR = 2.29	Pengxing Experimental School, Shenzhen, CLS = 57, FAR = 0.82	Tiandong Middle School, Shenzhen, CLS = 36, FAR = 1.02

Hybrid Layouts Teaching Building Cases			
			
Shixia School (South Campus), Shenzhen, CLS = 34, FAR = 1.67	Shenzhen Middle School (Nidgang Campus), CLS = 72, FAR = 1.00	Second Experimental School of Futian District, Shenzhen, CLS = 48, FAR = 1.05	Huafu Experimental School, Hongling Education Group, Shenzhen, CLS = 46, FAR = 2.39
			
The Affiliated Nansha Middle School, SCNU, CLS = 72, FAR = 0.70	Sino-Canada (Nanshan) International School, Shenzhen, CLS = 27, FAR = 0.95	Bao'an Experimental School, Shenzhen, CLS = 91, FAR = 0.91	Second Foreign Language School, Longhua District, Shenzhen, CLS = 54, FAR = 3.22

References

1. Su, C. Fragmentation of global public health governance: Problem analysis and strategic responses. *J. Yangtze Norm. Univ.* **2022**, *38*, 29.
2. Brown, T.M.; Wright, K.P., Jr. Opinion: How do we define 'healthy' lighting? *Light. Res. Technol.* **2022**, *54*, 310. [CrossRef]
3. Ministry of Education: Education Becomes the Largest Item in the General Public Budget. NetEase News. Available online: https://www.163.com/dy/article/HI942C5D0519DFFO.html (accessed on 10 May 2024).
4. Arrowstreet Inc. *Municipal and School Facilities Study and Master Plan*; Arrowstreet Inc.: Brockton, MA, USA, 2018; Volume 1—School Facilities Assessment.
5. Li, F.; Cui, Y.; Li, Y.; Guo, L.; Ke, X.; Liu, J.; Luo, X.; Zheng, Y.; Leckman, J.F. Prevalence of mental disorders in school children and adolescents in China: Diagnostic data from detailed clinical assessments of 17,524 individuals. *J. Child Psychol. Psychiatry* **2022**, *63*, 34–46. [CrossRef]
6. Lewy, A.J.; Kern, H.A.; Rosenthal, N.E.; Wehr, T.A. Bright artificial light treatment of a manic-depressive patient with a seasonal mood cycle. *Am. J. Psychiatry* **1982**, *139*, 1496–1498. [CrossRef]
7. Rosenthal, N.E.; Sack, D.A.; Gillin, J.C.; Lewy, A.J.; Goodwin, F.K.; Davenport, Y.; Mueller, P.S.; Newsome, D.A.; Wehr, T.A. Seasonal affective disorder: A description of the syndrome and preliminary findings with light therapy. *Arch. Gen. Psychiatry* **1984**, *41*, 72–80. [CrossRef]
8. Yang, J.; Ouyang, X.; Fu, H.; Hou, X.; Liu, Y.; Xie, Y.; Yu, H.; Wang, G. Advances in biomedical study of the myopia-related signaling pathways and mechanisms. *Biomed. Pharmacother.* **2022**, *145*, 112472. [CrossRef]
9. National Disease Control and Prevention Administration. The Myopia Rate Among Children and Adolescents in China Is on a Downward Trend. Available online: https://www.ndcpa.gov.cn/jbkzzx/c100010/common/content/content_1768152961235197952.html (accessed on 13 March 2024).
10. Hua, W.J.; Jin, J.X.; Wu, X.Y.; Yang, J.W.; Jiang, X.; Gao, G.P.; Tao, F.B. Elevated light levels in schools have a protective effect on myopia. *Ophthalmic Physiol. Opt.* **2015**, *35*, 252–262. [CrossRef]
11. Tao, R.; Yang, Z.G.; Wen, B.; Li, Y.H.; Dong, B.; Ma, J. Effects of classroom lighting environment improvement on vision of fourth-grade pupils. *Chin. J. Child Health Care* **2020**, *28*, 668.
12. Chen, R.; Jiang, H.; Bi, J.; Zhong, Y. Relationship between classroom daylighting and lighting conditions and poor vision among primary and secondary school students in Bao'an District, Shenzhen, from 2011 to 2014. *Prev. Med. Forum* **2016**, *22*, 131–133.
13. Ye, S.; Liu, S.; Cao, Y.; Wang, Q.; Zhang, X. Correlation between classroom lighting conditions and students' vision in primary and secondary schools in Tianjin. *Chin. J. Sch. Health* **2018**, *39*, 13–15.

14. Sun, B. Smart Lighting and Student Performance: A Novel System Design, Implementation, and Effects in Classrooms. Ph.D. Thesis, University of Waterloo, Waterloo, ON, Canada, 2021.
15. Zhang, X.; Tang, J.; Wang, Y.; Yang, W.; Wang, X.; Zhang, R.; Yang, J.; Lu, W.; Wang, F. Visual environment in schools and student depressive symptoms: Insights from a prospective study across multiple cities in eastern China. *Environ. Res.* **2024**, *258*, 119490. [CrossRef]
16. Bluyssen, P.M.; Zhang, D.; Kurvers, S.; Overtoom, M.; Ortiz-Sanchez, M. Self-reported health and comfort of school children in 54 classrooms of 21 Dutch school buildings. *Build. Environ.* **2018**, *138*, 106–123. [CrossRef]
17. Axarli, K.; Meresi, A. 211: Objective and Subjective Criteria Regarding the Effect of Sunlight and Daylight in Classrooms. In Proceedings of the PLEA, Dublin, Ireland, 22–24 October 2008.
18. Liu, Y.; Liu, B.; Wang, M. Exploration of adolescent educational space design based on the improvement of natural light environment. *Archit. Technol.* **2019**, *4*, 40–43.
19. Gao, W.; Zou, N.; Cao, F.; He, X.; Zhang, K.; Yang, M.; Li, J.; He, Q. Investigation of the current situation of classroom light environment in primary and secondary schools in northwest Guizhou and demonstration of on-site engineering renovation. *China Illum. Eng. J.* **2021**, *32*, 100–106.
20. Guan, Y.; Yan, Y. Research progress on dynamic classroom lighting to improve students' sub-health. *China Illum. Eng. J.* **2019**, *30*, 19–23.
21. Harley, R.K.; Lawrence, G.A.; Sanford, L.R.D.; Burnett, R. *Visual Impairment in the Schools*; Charles C Thomas Publisher: Springfield, IL, USA, 2000.
22. Wu, W.; Cao, Q. Preliminary field study on natural daylighting in school classrooms in Nanjing. *China Illum. Eng. J.* **2014**, *25*, 40–46.
23. Zhang, Y.; He, X.; Zou, N.; Cheng, M.; He, Q. Analysis of glare effects of classroom blackboard lighting. *China Illum. Eng. J.* **2020**, *31*, 140–144.
24. Lin, Z.; Gao, T.Y.; Vasudevan, B.; Ciuffreda, K.J.; Liang, Y.B.; Jhanji, V.; Fan, S.J.; Han, W.; Wang, N.L. Near work, outdoor activity, and myopia in children in rural China: The Handan offspring myopia study. *BMC Ophthalmol.* **2017**, *17*, 203. [CrossRef]
25. Huang, H.M.; Chang, D.S.T.; Wu, P.C. The association between near work activities and myopia in children—A systematic review and meta-analysis. *PLoS ONE* **2015**, *10*, e0140419.
26. Huang, C.J.; Tu, H.Y.; Hsueh, M.C.; Chiu, Y.H.; Huang, M.Y.; Chou, C.C. Effects of acute aerobic exercise on executive function in children with and without learning disability: A randomized controlled trial. *Adapt. Phys. Act. Q.* **2020**, *37*, 404–422. [CrossRef]
27. Zhou, H.; Bai, X. A review of the role of the school spatial environment in promoting the visual health of minors. *Int. J. Environ. Res. Public Health* **2023**, *20*, 1006. [CrossRef] [PubMed]
28. Ministry of Education, General Administration of Sport of China. Notice on Fully Launching the Nationwide Sunshine Sports Campaign for Hundreds of Millions of Students. Available online: http://www.gov.cn/gzdt/2007-04/26/content_599711.htm (accessed on 26 April 2007).
29. Ministry of Education of China. Results of the Eighth National Survey on Students' Physical Fitness and Health. Ministry of Education of China. Available online: http://www.gov.cn/xinwen/2021-09/03/content_5635317.htm (accessed on 3 September 2021).
30. Leslie, R.P. Capturing the daylight dividend in buildings: Why and how? *Build. Environ.* **2003**, *38*, 381–385. [CrossRef]
31. Leslie, R.P. *Patterns to Daylight Schools for People and Sustainability*; Lighting Research Center, Rensselaer Polytechnic Institute: Troy, NY, USA, 2010.
32. Guyon, D. Daylight Dividends Case Study: Smith Middle School, Chapel Hill, NC. *J. Green Build.* **2006**, *1*, 33–38. [CrossRef]
33. Innovative Design. Advancing Sustainable Design Since 1977—Innovative Design 2.0. Available online: https://www.innovativedesign.net/ (accessed on 10 May 2024).
34. WikiArquitectura. Corona School—Data, Photos & Plans. Available online: https://en.wikiarquitectura.com/building/corona-school/ (accessed on 10 May 2024).
35. Munkegaard School. Munkegaard School—Arne Jacobsen. Available online: https://arnejacobsen.com/works/munkegaard-school/ (accessed on 10 May 2024).
36. LEARN-INEU. Munkegaard School. Available online: https://learn-in.eu/munkegaard-school/ (accessed on 10 May 2024).
37. Bian, Y.; Ma, Y. Analysis of daylight metrics of side-lit room in Canton, south China: A comparison between daylight autonomy and daylight factor. *Energy Build.* **2017**, *138*, 347–354. [CrossRef]
38. Liu, Y.; Chen, K.; Deng, Q. Exploration of daylight-oriented profiles for high-density open-air classrooms based on MADRL. In *National Steering Committee for Architectural Education in Higher Education Institutions, Proceedings of the 2023 National Symposium on Architectural Digital Technology Teaching and Research: Digital Education and Intelligent Construction, 14 October 2023, Xiangtan, China*; Subcommittee for Architecture Education, Architectural Digital Technology Teaching Working Committee, Eds.; School of Architecture, South China University of Technology: Guangzhou, China, 2023; pp. 194–197. [CrossRef]
39. He, Y. Research on Natural Daylighting Design Methods for Primary and Secondary School Classrooms Based on Artificial Neural Networks and Genetic Algorithms. Ph.D. Thesis, South China University of Technology, Guangzhou, China, 2023. [CrossRef]

40. Huang, C.; Zhang, G.; Yao, J.; Wang, X.; Calautit, J.K.; Zhao, C.; An, N.; Peng, X. Accelerated environmental performance-driven urban design with generative adversarial network. *Build. Environ.* **2022**, *224*, 109575. [CrossRef]
41. Zhang, X.; Yang, L.; Luo, R.; Wu, H.Y.; Xu, J.; Huang, C.; Ruan, Y.; Zheng, X.; Yao, J. Estimating the outdoor environment of workers' villages in East China using machine learning. *Build. Environ.* **2022**, *226*, 109738. [CrossRef]
42. Le-Thanh, L.; Nguyen-Thi-Viet, H.; Lee, J.; Nguyen-Xuan, H. Machine learning-based real-time daylight analysis in buildings. *J. Build. Eng.* **2022**, *52*, 104374. [CrossRef]
43. Razmi, A.; Rahbar, M.; Bemanian, M. PCA-ANN integrated NSGA-III framework for dormitory building design optimization: Energy efficiency, daylight, and thermal comfort. *Appl. Energy* **2022**, *305*, 117828. [CrossRef]
44. Shi, C.; Han, Y.; Sun, C. Simulation and analysis of the thermal environment in complex atrium spaces in cold regions under natural ventilation conditions. *New Archit.* **2020**, *1*, 103–107.
45. Lorenz, C.L.; Spaeth, A.B.; Bleil De Souza, C.; Packianather, M.S. Artificial neural networks for parametric daylight design. *Archit. Sci. Rev.* **2020**, *63*, 210–221. [CrossRef]
46. Zhang, Z. Research on Multi-Scheme Generation of University Campus Layouts Based on Deep Learning. Ph.D. Thesis, South China University of Technology, Guangzhou, China, 2023. [CrossRef]
47. Li, D.G. Research on Generative Design of Architectural Layouts Under Multi-Objective Optimization. Ph.D. Thesis, Southeast University, Nanjing, China, 2025. [CrossRef]
48. Shi, Y. Computational Generation of Architectural Floor Plan Layouts Under Design Rules and Topological Constraints. Ph.D. Thesis, Southeast University, Nanjing, China, 2023. [CrossRef]
49. Lin, W. Research on Automatic Generation of Primary School Campus Design Layouts Based on Deep Learning. Ph.D. Thesis, South China University of Technology, Guangzhou, China, 2020. [CrossRef]
50. Lai, Y. Research on Generative Design of Architectural Layouts Based on pix2pix. Ph.D. Thesis, South China University of Technology, Guangzhou, China, 2021. [CrossRef]
51. Zhang, J. Exploration of Architectural Form and Space Generation Based on Multi-Agent Systems and Integer Programming Algorithms. Ph.D. Thesis, Southeast University, Nanjing, China, 2018.
52. Ma, C. Research on Generative Design of Primary and Secondary School Educational Buildings Based on Multi-Agent Systems. Ph.D. Thesis, South China University of Technology, Guangzhou, China, 2020. [CrossRef]
53. Liang, S. Computational Generative Study on Volumetric Design of Primary and Secondary School Buildings. Ph.D. Thesis, Harbin Institute of Technology, Harbin, China, 2020. [CrossRef]
54. Wallacei. Evolutionary Engine for Grasshopper3D | Wallacei: An Evolutionary Multi-Objective Optimization Analytic Engine for Grasshopper, 3D. Available online: https://www.wallacei.com/ (accessed on 10 May 2024).
55. Macken, Y. Rhino-Hops-Backend. GitHub. Available online: https://github.com/yannickmacken/rhino-hops-backend (accessed on 12 May 2024).
56. Guangzhou Municipal Government. Guangzhou Plans to Add 70,000 Public Basic Education Places This Year. Available online: https://www.gz.gov.cn/zwfw/zxfw/jyfw7/content/post_9858792.html (accessed on 9 September 2024).
57. Guangzhou Municipal Education Bureau; Guangzhou Municipal Planning and Natural Resources Bureau; Guangzhou Municipal Housing and Urban-Rural Development Bureau. *Guidelines for the Construction Standards of Ordinary Primary and Secondary Schools in Guangzhou*; Guangzhou Municipal People's Government: Guangzhou, China, 2022.
58. Ministry of Construction of the People's Republic of China. *Standards for the Construction of School Buildings in Ordinary Primary and Secondary Schools in Urban Areas*; China Planning Press: Beijing, China, 2002.
59. Department of Education of Guangdong Province. *Standards for Standardized Schools of Compulsory Education in Guangdong Province*; Guangdong Provincial People's Government: Guangzhou, China, 2017.
60. Department of Education of Guangdong Province. *Implementation Measures for the Curriculum of Compulsory Education in Guangdong Province*, 2024th ed.; Guangdong Provincial People's Government: Guangzhou, China, 2024.
61. Liu, B.; Liu, Y.; Deng, Q.; Hu, K. A study on daylighting metrics related to the subjective evaluation of daylight and visual comfort of students in China. *Energy Build.* **2023**, *287*, 113001. [CrossRef]
62. *GB 55016-2021*; General Code for Building Environment. China Architecture & Building Press: Beijing, China, 2021.
63. *EN 17037:2018*; British Standards Institution. Daylight in Buildings. BSI Standards Limited: London, UK, 2019.
64. *IES LM-83-12*; IES Spatial Daylight Autonomy (sDA) and Annual Sunlight Exposure (ASE). Illuminating Engineering Society: New York, NY, USA, 2012.
65. US Green Building Council. *LEED v4.1 Interior Design and Construction: Getting Started Guide for Beta Participants*; U.S. Green Building Council: Washington, DC, USA, 2020.
66. *GB/T 50785-2023*; Evaluation Standard for Indoor Thermal and Humidity Environment of Civil Buildings. China Architecture & Building Press: Beijing, China, 2023.
67. Yang, L.; Shami, A. On hyperparameter optimization of machine learning algorithms: Theory and practice. *Neurocomputing* **2020**, *415*, 295–316. [CrossRef]

68. Shahriari, B.; Swersky, K.; Wang, Z.; Adams, R.P.; De Freitas, N. Taking the human out of the loop: A review of Bayesian optimization. *Proc. IEEE* **2015**, *104*, 148–175. [CrossRef]
69. Deb, K.; Pratap, A.; Agarwal, S.; Meyarivan, T.A.M.T. A fast and elitist multiobjective genetic algorithm: NSGA-II. *IEEE Trans. Evol. Comput.* **2002**, *6*, 182–197. [CrossRef]
70. Myers, J.L.; Well, A.D.; Lorch, R.F., Jr. *Research Design and Statistical Analysis*; Routledge: Abingdon-on-Thames, UK, 2013.
71. Akiba, T.; Sano, S.; Yanase, T.; Ohta, T.; Koyama, M. Optuna: A next-generation hyperparameter optimization framework. In Proceedings of the 25th ACM SIGKDD International Conference on Knowledge Discovery & Data Mining, Anchorage, AK, USA, 4–8 August 2019; pp. 2623–2631.
72. Al-Douri, F. Integrated BIM+ Parametric Modelling: A decision-support tool for human-centric campus simulation, automation, and optimization. *Ekistics New Habitat* **2024**, *84*, 56–64. [CrossRef]
73. Sun, C.; Liu, Q.; Han, Y. Many-objective optimization design of a public building for energy, daylighting and cost performance improvement. *Appl. Sci.* **2020**, *10*, 2435. [CrossRef]
74. Gassar, A.A.A.; Koo, C.; Kim, T.W.; Cha, S.H. Performance optimization studies on heating, cooling and lighting energy systems of buildings during the design stage: A review. *Sustainability* **2021**, *13*, 9815. [CrossRef]
75. Dong, Y.; Sun, C.; Han, Y.; Liu, Q. Intelligent optimization: A novel framework to automatize multi-objective optimization of building daylighting and energy performances. *J. Build. Eng.* **2021**, *43*, 102804. [CrossRef]
76. Leng, S.; Lin, J.R.; Li, S.W.; Hu, Z.Z. A data integration and simplification framework for improving site planning and building design. *IEEE Access* **2021**, *9*, 148845–148861. [CrossRef]
77. Fang, Y.; Cho, S. Design optimization of building geometry and fenestration for daylighting and energy performance. *Sol. Energy* **2019**, *191*, 7–18. [CrossRef]
78. Atthaillah, A.; Mangkuto, R.A.; Koerniawan, M.D.; Hensen, J.L.; Yuliarto, B. Optimization of daylighting design using self-shading mechanism in tropical school classrooms with bilateral openings. *J. Daylighting* **2022**, *9*, 117–136. [CrossRef]
79. Marinelli, L.J.; Annunziata, A.; Caselli, B.; Desogus, G.; Torrisi, V.; Garau, C. Accessibility and Polarities of Pedestrian Network in University Campuses. A Space Syntax Application. In *International Conference on Computational Science and Its Applications*; Springer Nature: Cham, Switzerland, 2023; pp. 383–400.
80. Günaydın, A.S.; Yücekaya, M. An investigation of sustainable transportation model in campus areas with space syntax method. *ICONARP Int. J. Arch. Plan.* **2020**, *8*, 262–281. [CrossRef]
81. Pan, Z.G.; Lan, G.W.; Fan, D.L.; Du, Y.L.; Zeng, Y. Analysis of accessibility of urban roads based on space syntax and distance measurement. *Int. Arch. Photogramm. Remote Sens. Spat. Inf. Sci.* **2020**, *42*, 159–165. [CrossRef]
82. Liu, J.; Wu, X.; Wang, B.; Wu, Q.; Tian, L. Simulation of light environment in a serrated photovoltaic greenhouse and optimization of daylighting roofs based on Design Builder. *Trans. Chin. Soc. Agric. Eng.* **2025**, *41*, 211.
83. Körmeçli, P.Ş. Evaluating accessibility of street network in neighborhood by space syntax method: The case of Çankırı. *ICONARP Int. J. Archit. Plan.* **2023**, *11*, 625–649. [CrossRef]
84. Fakhr, B.V.; Mahdavinejad, M.; Rahbar, M.; Dabaj, B. Design optimization of the skylight for daylighting and energy performance using NSGA-II. *J. Daylighting* **2023**, *10*, 72–86. [CrossRef]
85. Gao, Y.; Zhao, S.; Huang, Y.; Pan, H. Multi-Objective Optimization of Daylighting–Thermal Performance in Cold-Region University Library Atriums: A Parametric Design Approach. *Energies* **2025**, *18*, 1184. [CrossRef]
86. Costanzo, V.; Evola, G.; Marletta, L. A review of daylighting strategies in schools: State of the art and expected future trends. *Buildings* **2017**, *7*, 41. [CrossRef]
87. Yang, X.; Wang, J.; Guo, J. A Study on Natural Lighting Design Strategies for Teaching Buildings in Hot-summer and Cold-winter Zone of China—A case of the Arts and Sciences Building of Xinyang Normal University. In Proceedings of the 7th International Building Physics Conference, IBPC2018, Syracuse, NY, USA, 23–26 September 2018.
88. Heschong, L.; Wright, R.L.; Okura, S. Daylighting impacts on human performance in school. *J. Illum. Eng. Soc.* **2002**, *31*, 101–114. [CrossRef]

Disclaimer/Publisher's Note: The statements, opinions and data contained in all publications are solely those of the individual author(s) and contributor(s) and not of MDPI and/or the editor(s). MDPI and/or the editor(s) disclaim responsibility for any injury to people or property resulting from any ideas, methods, instructions or products referred to in the content.